

THE VIRGO CLUSTER DISTANCE FROM 21 CM-LINE WIDTHS

Martin Federspiel, G.A. Tammann

Astronomisches Institut der Universität Basel, Venusstr. 7, CH-4102 Binningen, Switzerland

Allan Sandage

The Observatories of the Carnegie Institution of Washington, 813 Santa Barbara Street,
Pasadena, CA 91101

ABSTRACT

The distance of the Virgo cluster is derived in the B band from the 21 cm-line width-absolute magnitude relation. The latter is calibrated using 18 spirals with Cepheid distances mainly from HST. The calibration is applied to a *complete* sample of non-peculiar spirals with $i > 45^\circ$ and lying within the optical (n=49) or X-ray (n=35) contour of the cluster, resulting in a mean cluster distance of $(m - M)^0 = 31^m58 \pm 0^m24$ (external error) or 20.7 ± 2.4 Mpc. The mean distance of subcluster A is $0^m46 \pm 0^m18$ smaller than that of subcluster B, but the individual distances of the members of the two substructures show considerable overlap. Cluster spirals with $30^\circ < i < 45^\circ$ yield almost as good distances as more inclined galaxies. HI-truncated galaxies are overluminous by 0^m8 at a given line width. The distance modulus is corrected by -0^m07 for the fact that cluster members have lower HI-surface fluxes and are redder in $(B - I)$ at a given line width than the (field) calibrators. Different sources of the B magnitudes and line widths have little effect on the resulting distance. Different precepts for the internal-absorption correction change the result by no more than $\pm 0^m17$. The individual distances of the cluster members do not show any dependence on recession velocity, inclination, Hubble type or line width. The dependence on apparent magnitude reflects the considerable depth effect of the cluster. The adopted distance is in good agreement with independent distance determinations of the cluster.

Combining the cluster distance with the corrected cluster velocity of 1142 ± 61 km s^{-1} gives $H_0 = 55 \pm 7$ km s^{-1} Mpc $^{-1}$ (external error). If the Virgo cluster distance is inserted into the tight Hubble diagram of clusters out to 11 000 km s^{-1} using *relative* distances to the Virgo cluster one obtains a global value of $H_0 = 57 \pm 7$ km s^{-1} Mpc $^{-1}$.

Subject headings: Virgo cluster – distance scale – Hubble constant – Tully-Fisher relation

1. Introduction

The correlation of the rotational velocity and the luminosity of a galaxy was first exploited by Öpik (1921, 1922) in papers well ahead of their time. Subsequently Gougenheim (1969)

suggested 21 cm line widths to be used as a measure of the rotational velocity and hence of the galaxy luminosity. The ensuing 21 cm-line width-absolute magnitude relation of the form

$$M = a \log w + b \tag{1}$$

is now known as “Tully-Fisher”(TF) relation (Tully & Fisher 1977).

The first application of the TF method to the Virgo cluster gave a distance modulus of $(m - M) = 31.70 \pm 0.08$ (Sandage & Tammann 1976). This relatively large value was confirmed by Kraan-Korteweg, Cameron & Tammann (1988) and, after correction of the distances of the local calibrators, by Fouqué et al. (1990) using a *complete* cluster sample. Incomplete cluster samples, however, have consistently given significantly smaller TF distances (Aaronson, Huchra, & Mould 1979, Pierce & Tully 1988). This is now understood as the result of the Teerikorpi cluster effect (Teerikorpi 1984, 1987, 1990, 1993; Sandage, Tammann & Federspiel 1995), which always leads to too small distances if an incomplete set of cluster galaxies is used to define the slope of the TF relation (cf. Fig. 13 below) or of any other relation between an observational parameter and the absolute magnitude in the presence of intrinsic scatter.

Justification for a re-examination of the TF distance comes from several facts. (1) The calibration of the TF relation can now be based on an unprecedented sample of spiral galaxies with Cepheid distances mainly from HST, and a complete sample of cluster spirals can now objectively be selected from optical as well as X-ray surveys (Sects. 2 and 5.3). (2) The resulting zero-point of the TF relation is firm (Sect. 2.1) and the mean distance of a complete sample of 49 inclined Virgo spirals carries a correspondingly small systematic and statistical error (Sect. 5). Largely independent data sets and different correction procedures allow an assessment of the influence of varying the input parameters (Sect. 6). Several tests (Sect. 7) are used to demonstrate the internal consistency of the individual galaxy distances. In Sect. 8 we investigate the difference between the calibrators and the Virgo spirals in HI surface brightness and $(B - I)$ color and its effect on the derived distances. The spatial structure of the Virgo cluster as outlined by the TF distances is illustrated in Sec. 9. The discussion in Sect. 10 compares the results with external data. The conclusion with respect to H_0 are presented in Sect. 11.

2. Sample Selection

2.1. Calibrators

During the last few years the number of galaxies with Cepheid distances has been growing significantly due to the capabilities of the Hubble Space Telescope. For the first time there are enough galaxies with Cepheid distances for a reliable calibration of the TF relation. We use 18 spirals of Hubble types $T = 2$ to 5 of which 12 have Cepheid distances determined with HST, and 4 have ground-based Cepheid distances set out later in Table 2. Two late-type members ($T = 7$) of the tight M 101 group (NGC 5204 and NGC 5585) without individual Cepheid distance were

added to extend the range of Hubble types of the sample. These two galaxies were assigned the HST-Cepheid distance of M101. We consider the M81 and the Sculptor group to be too spread in distance and do not include members of these groups without individual Cepheid distances. NGC 4496A, which has a Cepheid distance (Saha et al. 1996a), is not used because its total magnitude is disturbed by NGC 4496B.

The zeropoint of the P-L relation of Madore & Freedman (1991) which we have used rests on the assumption that the true distance modulus of LMC is $(m - M)^0 = 18^m50$. Eleven distance determinations based on geometrical, physical and astronomical zeropoints give consistently $(m - M)^0 = 18^m56 \pm 0^m03$ shown in Table 1. If this value is taken at face value, the derived Virgo cluster modulus would increase by $0^m06 \pm 0^m03$, and H_0 would be decreased by $\sim 3\%$ from the value we derive in Sect. 11. In addition, the majority of the Cepheid distances of the calibrators in Table 2 are taken from the original literature, i. e. they are not corrected for the long-exposure effect of the WFPC2 (Saha et al. 1996b; Hill et al. 1997). This effect would increase the Cepheid distances of several galaxies by another 0^m05 and decrease H_0 by another $\sim 2\%$. On the other hand Tanvir (1997) has pointed out a slight inconsistency of the I magnitudes used by Madore & Freedman (1991) affecting the Cepheid distances determined from V and I magnitudes with HST. He proposes H_0 to be larger by 5% for this effect; since 13 out of 18 calibrators in Table 2 depend on V and I data from HST this causes a 3-4% increase of the adopted value of H_0 in Sect. 11. This should approximately be balanced by a somewhat higher LMC modulus in Table 1 and the long-exposure effect. In addition there is at least the suspicion that HST photometry in crowded fields gives too *bright* magnitudes (Sodemann & Thomson 1997); for the relevant Cepheids the effect is estimated to be $\sim 0^m05$ which leads to a corresponding underestimate of the distances (Saha & Labhardt 1997).

In a preprint C.S. Kochanek (1997) has calculated Cepheid distances of 15 galaxies relative to LMC [again assumed to be at $(m - M)^0 = 18^m50$] by combining all available multi-color Cepheid data and assuming that they are strictly on a homogeneous photometric system and have equal weight. Actually, the mean V and I magnitudes from HST, for instance, have grossly different errors, because the former are based on a sufficient number of observations, but the latter only on a bare minimum. Moreover, the I magnitudes are measured against stronger background effects. If a period-luminosity-color (PLC) relation is used, as the author proposes, the necessarily large errors in $(V - I)$ or any other color are multiplied by the coefficient of the color term of roughly 2.5 (depending on wavelength). A yet more fundamental objection against the simple ansatz of a PLC relation has since been raised by Saio & Gautschy (1997) who find a strong variation of the slope of the constant-period lines depending on the period. Kochanek offers four different model solutions for the distance moduli, none of which is fully self-consistent. His solutions make the calibration in eq. (3) 0^m14 fainter on average. Yet we see no merit in these solutions.

It remains the question of the metallicity dependence of the Cepheid distances. Important effects have been proposed (e.g. Sasselov et al. 1997; Beaulieu & Sasselov 1996; Sekiguchi & Fukugita 1997). On the other hand Madore & Freedman (1991) and Böhm-Vitense (1997) have

given observational evidence against a metallicity dependence. The most direct observational evidence comes from the metal-rich Galactic and the metal-deficient LMC Cepheids; the former as calibrators yield an LMC Cepheid distance in agreement with evidence that is independent of Cepheids (Table 1). Also Di Benedetto (1997) has derived Cepheid distances including the metal poor SMC, and has obtained fully consistent results *independent* of wavelength. The question comes now to rest with fully theoretical treatments of stellar evolution coupled with pulsational theory indicating that the dependence of M_{bol} on $\log P$ is surprisingly insensitive to metallicity (Stothers 1988; Chiosi, Wood, & Capitanio 1993; Sandage 1996c; Saio & Gautschy 1997). Allowing for the metal dependence of the bolometric correction introduces at a given $\log P$ a variation of M_V and of $< 0^m1$ over the relevant metallicity range.

The *slope* of the P-L relation of LMC is quite well determined in different wavelengths (Madore & Freedman 1991). Any remaining uncertainties of the slope have a minute effect on the derived distances. The period range of the Cepheids used for the calibrators in Table 2 is sufficient to minimize selection effects (Sandage 1988); in any case they can only lead to an underestimation of the distances.

For these reasons it appears that any *systematic* errors of the Cepheid distances of the calibrators in Table 2 are below 0^m10 .

2.2. Virgo spiral galaxies

The Virgo Cluster Catalogue (VCC; Binggeli, Sandage, & Tammann 1985) is the main base from which we selected the different samples of Virgo spirals. The present investigation is restricted to Hubble types 2 to 8 (Sab to Sdm), because none of the calibrators is of type 1 (Sa), and because late-type galaxies (type 9 and 10) have exceptionally uncertain inclinations i . The VCC contains 151 spirals of types 2 to 8 with $v_0 < 2600 \text{ km s}^{-1}$. Of these 98 (123) have $i > 45^\circ (30^\circ)$, generally considered to be a necessary condition to confine the inclination corrections of the observed line width. Binggeli, Popescu, & Tammann (1993) assigned memberships in subgroups to many of the VCC galaxies. 34 “normal” spirals with $i > 45^\circ$ in the notation of Binggeli et al. (1993) belong to subgroup “big A” around M87, 15 are members of subgroup “B ($r = 2.4^\circ$)”, i.e. they lie within 2.4° of M49. The corresponding numbers for galaxies with $i > 30^\circ$ are 48 and 19, respectively. For these galaxies photometric as well as HI data are available from different sources. We define these 34 “inner” spirals of A and the 15 “inner” spirals of B with $i > 45^\circ$ as our “fiducial sample”. The qualification “normal” is to mean that they are not classified as “peculiar” (Binggeli et al. 1985) and that they are not HI-truncated (Guhathakurta et al. 1988). The “fiducial sample” is identified in Table 3. The 5 HI-truncated and the 2 (5) peculiar spirals with $i > 45^\circ (30^\circ)$ are listed next in Table 3. Also listed are the 15 spirals which fall within the X-ray contours of the cluster but outside of A and B. All spirals of the “fiducial sample” are considered to be members of the Virgo cluster. This assignment will be tested below. Finally, Table 3 contains 41 galaxies which lie outside A and B and outside the X-ray contours.

Of these 15 lie outside the field of the VCC and were added from other Virgo samples (Fouqué et al. 1990; Kraan-Korteweg et al. 1988; Pierce and Tully 1988). The projected positions of all the 103 non-peculiar spirals with $i > 45^\circ$ is shown in Fig. 1.

3. Observational Data

3.1. Calibrators

The observational parameters of the calibrators and their sources are given in Table 2. The columns have the following meaning:

1. name in the NGC catalogue
2. Hubble type as given by the RSA (Sandage & Tammann 1987) in the nomenclature of the RC3 (de Vaucouleurs et al. 1991)
3. total apparent B magnitude corrected for internal and Galactic absorption as listed in the RC3 [based on the maps of Burstein & Heiles (1984)]
4. correction for internal absorption calculated from the Hubble type [column (2)] and $\log R_{25}$ following the RC3 scheme
5. correction for Galactic absorption as listed in the RC3
6. adopted true distance modulus
7. source for (6):
 - 1 Madore & Freedman (1991)
 - † Böhm-Vitense (1997) gives a Cepheid modulus of $(m - M)_{M31} = 24.67$ if $(m - M)_{LMC} = 18.50$
 - 2 Silbermann et al. (1996a)
 - 3 Silbermann et al. (1996b)
 - 4 Sakai et al. (1996)
 - 5 Freedman & Madore (1994)
 - 6 Graham et al. (1996)
 - 7 Tanvir et al. (1995)
 - 8 Macri et al. (1996)
 - 9 Ferrarese et al. (1996)
 - 10 Saha et al. (1996b)

- 11 Sandage et al. (1996)
 - 12 Kelson (1996)
 - 13 Hughes (1996)
8. absolute B magnitude calculated from (3) and (6)
 9. adopted error in the absolute magnitude [combined from the respective errors of the distance modulus as listed in the original source, an assumed error of $0^m.1$ in the photometry and an assumed error of $0.2(A^i + A^0)$]
 10. inclination calculated from $\log R_{25}$ as listed in the RC3 following Fouqué et al. (1990);
* adopted inclinations are $i = 29^\circ$ for N 4321 (mean from Grosbøl 1985, Warmels 1988, Arsenault et al. 1988, Pierce 1994) and $i = 22^\circ$ for N 5457 (mean from Rogstad & Shostak 1972, Comte, Monnet, & Rosado 1979, Bosma, Goss, & Allen 1981, Pierce 1994)
 11. log HI line width read at the 20% level, corrected for inclination and turbulent motions and motions in z -direction (in most cases copied from Huchtmeier & Richter 1988, 1989)
 12. log HI linewidth read at the 20% level, corrected for inclination and turbulent motions and motions in z -direction, calculated from w_{20} given by LEDA. Inclinations for the edge-on corrections were taken from column (9) and the correction for turbulent motion and the motion in z -direction was calculated following Huchtmeier & Richter (1989).
 13. uncertainty in log HI linewidth composed of the assumed uncertainties of the measured linewidth w_{20} and the inclination of column (10), i.e. 10 km s^{-1} and 5° , respectively.

3.2. Virgo spiral galaxies

The data for the Virgo sample galaxies are listed in Table 3. The columns have the following meaning:

1. Name as listed in one of the following catalogs: NGC (N), IC (I), UGC (U), VCC (V), ZWG (Z)
2. Virgo subgroup membership as assigned by Binggeli et al. (1993); Y means that the galaxy does not lie in VCC field but is included in the samples of other authors; spirals with code Z are not assigned a subgroup membership; X means member of the X-ray sample (the projected position is within the defining X-ray isophote; cf. Sect. 5.3)
3. Hubble type as listed in the VCC on the scheme of the RC3
4. total apparent B_T magnitude from RC3, corrected for internal and Galactic absorption as given in columns (6) and (8)

5. uncertainty in $B_T^{0,i}$ composed of the assumed errors of the photometry and of the internal and Galactic absorption corrections, i. e. 0^m1 and $0.2(A^i + A^0)$, respectively; for the fit of the TF relation we assume in addition an uncertainty of 0^m2 to make some allowance for the depth effect of the cluster.
6. correction for internal absorption calculated for the Hubble type listed in column (3) and $\log R_{25}$ as given in the RC3 following the RC3 scheme
7. correction for internal absorption as given in the RSA
8. A^0 correction for Galactic absorption as given in the RC3 [based on the maps of Burstein & Heiles (1984)]
9. inclination calculated from $\log R_{25}$ as listed in the RC3 following the recipe of Fouqué et al. (1990)
10. \log HI line width read at the 20% level, corrected for inclination and turbulent motions and motions in z -direction, taken from Huchtmeier and Richter (1989). An asterisk denotes the cases where $\log w$ had to be calculated from w_{20} listed in the RC3. Two asterisks indicate those cases where $\log w$ was computed from w_{20} given by Hoffman et al. (1987, 1989). Cases for which no HI data were available are marked with a dagger.
11. \log HI line width read at the 20% level, corrected for inclination and turbulent motions and motions in z -direction, calculated from w_{20} given by LEDA. Inclinations were taken from column (9) and the correction for turbulent motion and the motion in z -direction was calculated following Huchtmeier & Richer (1989).
12. uncertainty in \log HI linewidth composed of the assumed uncertainties of the measured linewidth w_{20} and the inclination of column (9), i.e. 10 km s^{-1} and 5° , respectively.

4. The calibrated Tully-Fisher relation

A first solution of the calibration of the Tully-Fisher relation was obtained by fitting a straight line to the absolute magnitudes (as the dependent variable) and line widths (as the independent variable) of the calibrators listed in Table 2, columns (8) and (12). Each calibrator was weighted with its estimated error of M_B (column 9 of Table 2). The result of this free fit is:

$$M_B = (-6.32 \pm 0.08) \log w - (4.05 \pm 0.19) \quad \sigma_M = 0^m43. \quad (2)$$

A second solution is presented taking the errors in magnitude *and* line width into account. This is achieved by dropping slanted lines with slope ϵ_y/ϵ_x onto a regression line and demanding a least squares minimalization (cf. Seares 1944). For this the BCES (Bivariate Correlated measurement Errors and intrinsic Scatter) algorithm of Akritas, Bershady & Bird (1996) is used. The adopted

errors on both axes are taken from columns (9) and (13) of Table 2 and from columns (5) and (12) in Table 3. Since the slope of the TF relation is determined much better by including the 49 members of the “fiducial Virgo sample” described in Sect. 2.2 we combine the sample of the calibrators with the Virgo sample assuming different distance moduli and search for that solution which gives a minimum value of the merit function χ^2 .

We obtain the following relation which is illustrated in Fig. 2:

$$M_B = (-6.97 \pm 0.02) \log w - (2.35 \pm 0.05). \quad (3)$$

The slope of eq. (3) is somewhat steeper than the slope of eq. (2), a consequence of now including the errors in $\log w$.

We adopt eq. (3) as our reference and discuss the influence of different input parameters in Sect. 6. The effect of the remaining uncertainty of the slope is discussed in Sect. 10.

It is of some theoretical interest to determine the intrinsic scatter of the TF relation. Taking the observed magnitude scatter about eq. (3) of $\sigma_M = 0^m44$ from the calibrator sample and subtracting the typical error in M of the calibrators, i.e. 0^m25 , and the error introduced by the mean adopted errors in line width, which translate to $\sigma_{M(w)} = 0^m28$, gives an intrinsic scatter of $\sigma_M = 0^m23$. In the presence of unavoidable errors of the input parameters this value is, of course, meaningless for practical applications.

5. The Virgo cluster distance

In this section the TF distances to different Virgo samples are discussed.

5.1. A first approximation

The direct TF relation allowing only for errors in magnitude [Table 3, columns (4) and (5)] gives for the “fiducial sample” defined in Sect. 2.2

$$m_B = (-6.60 \pm 0.03) \log w + (28.31 \pm 0.06) \quad \sigma_M = 0^m57. \quad (4)$$

and combined with eq. (2) gives a distance modulus of $(m - M) = 31^m62 \pm 0^m08$. We prefer, however, the solution which takes into account the errors in magnitude *and* line width. In this case a χ^2 method (cf. Sect. 4) gives

$$(m - M) = 31^m50 \pm 0^m09. \quad (5)$$

The data were weighted with their individual errors in magnitude and line width. This value is further discussed in Sects. 6.5 and 8. The finally adopted value and its error are given in Sect. 10.

If the spirals in Fig. 3 are subdivided into subclusters A and B a significant distance difference of $\Delta(m - M) = 0^m46 \pm 0^m18$ emerges (cf. Schröder 1996). This raises several problems. The distance difference is small enough and the distance overlap between individual galaxies so pronounced (cf. Figs. 11 and 12 below) that the two subgroups must be gravitationally bound as is also shown by their common X-ray contour (cf. Fig. 4 below). Moreover, the distance difference is *not* confirmed by other relative distance indicators. $D_n - \sigma$ data (Faber et al. 1989) for 11 galaxies in A in B suggest A to be *more* distant than B by $0^m05 \pm 0^m36$; two blue SNe Ia and one in B give $\Delta(m - M) = +0^m55 \pm \sim 0^m3$ again in the sense of A being more distant. The apparent magnitude of NGC 4472 (M 49), the brightest galaxy in B, is already brighter than that of NGC 4486 (M 87) in subgroup A which has all the properties expected of a brightest cluster galaxy; if B is assumed to be more distant than A the *absolute* magnitude of NGC 4472 becomes excessively bright as compared to NGC 4486. Not attempting here to understand the complex spatial structure of the cluster, we must adopt for practical reasons a mean distance of the spirals in subgroup A *and* B because all previous workers in the field have done so. In particular, the Hubble diagram with cluster distances relative to the Virgo cluster (Fig. 14 below) is based on the *entire* Virgo sample.

The “fiducial sample” contains only galaxies with inclinations $> 45^\circ$ to avoid possibly large errors in the calculation of true line widths from the observed line widths. If an inclination limit of $i > 30^\circ$ is admitted instead of $i > 45^\circ$, the sample is increased from 49 to 67 “normal” members in subgroups A and B. This increased sample gives instead of eq. (5)

$$(m - M) = 31^m48 \pm 0^m07. \quad (6)$$

The TF slope of the combined samples (Virgo [$i > 30^\circ$] and calibrators) is -7.15 . The effect of the less inclined galaxies on the distance modulus is surprisingly small.

The Virgo cluster modulus is further discussed in the following subsections and in Sect. 6.

5.2. The influence of HI-truncated and peculiar galaxies on the TF distance

There are five galaxies in subgroup A which have an unusually small HI disk (Guhathakurta et al. 1988). These galaxies were excluded from the “fiducial sample”. If the HI-stripped objects listed in Table 3 were included into the calculation of the TF distance of the fiducial sample one would obtain $(m - M) = 31^m43 \pm 0^m09$. To show the effect even more drastically: the mean distance of the HI-stripped galaxies *alone* with the calibration of eq. (3) is $(m - M) = 30^m81 \pm 0^m24$. Figure 3 shows that the HI-truncated galaxies are $\sim 0^m8$ *too luminous for their line width*. We conclude that it is not appropriate to use HI-truncated galaxies in the TF relation. Distances to samples with HI truncated galaxies are underestimated.

The same conclusion holds for the two galaxies of the fiducial sample which are classified as peculiar or interacting from their morphological appearance. With a mean $(m - M) = 31^m14 \pm 0^m21$ they also tend to give too small distances. They were therefore excluded from our analysis.

5.3. The distance of the Virgo X-ray sample

The diffuse X-ray emission of the hot gas in the Virgo cluster has been measured by ROSAT (Böhringer et al. 1994). We use the X-ray boundary, i.e. the isophote with $0.444 \text{ counts s}^{-1} \text{ arcmin}^{-1}$ as an *independent* mean to define the cluster population (Fig. 4). There are 42 galaxies with $i > 45^\circ$ within the defining X-ray contours (HI-truncated and peculiar objects omitted). The fact that the south-east side of the X-ray contour is disturbed by the Galactic North Polar Spur has only negligible effect on the sample selection.

Combining both the calibrator and the X-ray samples and taking errors both in magnitudes and $\log w$ into account gives a TF slope of -6.55 , which is slightly but insignificantly shallower than that found in eq. (3). The distance modulus of the X-ray sample corresponding to this solution is

$$(m - M) = 32^m05 \pm 0^m11, \quad \sigma_{(m-M)} = 0^m70. \quad (7)$$

The distance is 0^m55 larger than the distance of the optically selected “fiducial sample”. The difference is partly due to the seven galaxies in the X-ray sample which are assigned to the W and W’ cloud (lying in or near the lower right “peninsula” of the defining X-ray isophote in Fig. 4). The latter have a mean recession velocity of $v_{\text{LG}} = 1645 \text{ km s}^{-1}$ and give a TF distance modulus of $(m - M) = 32^m58 \pm 0^m20$. The X-ray sample without these seven galaxies yields

$$(m - M) = 32^m00 \pm 0^m11 \quad \sigma_{(m-M)} = 0^m68. \quad (8)$$

Even after exclusion of the seven galaxies the distance modulus is relatively high. The reason is the shallower slope of the TF relation of the X-ray sample as compared to the fiducial sample. Shallower slopes always tend to increase the distance.

5.4. The distances of Virgo galaxies outside the “fiducial sample” and outside the X-ray sample

If the adopted TF relation (eq. 3) is applied to the 38 galaxies of Table 3 which are not members of the fiducial sample or the X-ray sample, one obtains a large mean distance modulus of $(m - M) = 31^m85$ with a large dispersion of $\sigma_{(m-M)} = 1^m05$. Indeed, Binggeli et al. (1993) assigned some of these outlying members to the M, W, W’ or S clouds, which appear to be in the background for morphological and other reasons.

The individual TF distances of the outlying galaxies are plotted versus recession velocity in Fig. 5. The qualitative difference to Fig. 6 below is obvious. Some nearby and several distant galaxies are probably not cluster members. They seem to partake in the (nearly) free expansion field.

6. The influence of different data sources on the TF distance of the Virgo cluster

The influence of different input parameters on the distance of the Virgo cluster is now investigated.

6.1. Using alternative B magnitudes

The distance of the Virgo cluster does not change when magnitudes from different sources are used. Replacing the B_T magnitudes in Table 3, column 4 by those of Schröder (1996), but keeping the RC3 corrections, increases the distance modulus by only 0^m04 . Using instead the magnitudes of Yasuda, Fukugita, & Okamura (YFO 1997), again with the RC3 corrections, gives a very similar modulus of $(m - M) = 31^m49$ for the fiducial sample.

6.2. Using an alternative set of line widths

Huchtmeier & Richter (1988, 1989) have published HI data for nearby galaxies and galaxies in the Virgo cluster. Their line widths can be used as an alternative data set to the w_{20} data of the Lyon Extragalactic Data Base (LEDA). The two sets of w_{20} line widths usually are in good agreement, although there is an average systematic offset of $+6 \text{ km s}^{-1}$, the Huchtmeier & Richter values being larger. Using the fully reduced Huchtmeier & Richter data for the calibrators as well as for the Virgo spirals gives the same distance within 0^m09 as eq. (5). However, the dispersion of the TF relations for both the calibrators and the Virgo galaxies is slightly enlarged (Table 4, solution 2).

6.3. Using an alternative scheme for internal absorption

So far the corrections for internal absorption were taken from the RC3. Alternative precepts to determine the internal-absorption corrections are given in the RSA (Sandage & Tammann 1987). The main difference is that the RC3 corrects the magnitudes to face-on orientation, while the RSA allows for the *total* internal absorption. In addition the RSA corrections have a somewhat stronger dependence on Hubble type. As seen from Table 4 for solutions 5 and 6, the internal absorption corrections of the RSA lead to a slightly steeper slope of the TF relation and to an insignificantly larger scatter. Also the Virgo modulus is $\sim 0^m17$ larger. However, the individual TF distances are equally consistent as those with the RC3 correction, i. e. they do not correlate significantly with Hubble type, line-width, nor inclination (cf. Sect. 7). The modulus difference between subclusters A and B remains at 0^m46 .

It has often been proposed to use infrared magnitudes for the TF relation to circumvent the relatively large intrinsic-absorption corrections in B . However, the absorption in the I -band is

still much larger than a $1/\lambda$ -law would suggest (Schröder 1996; Giovanelli et al. 1994). Moreover, the modest advantage of the smaller absorption is offset by the steeper slope of the I -band TF relation (for a discussion cf. Schröder 1996).

6.4. Corrections for Galactic absorption

Since the Galactic latitude of the Virgo cluster is $60^\circ < b < 80^\circ$ the influence of Galactic absorption is small or negligible. Maps of the HI column density indicate that the Galactic absorption is not zero for all Virgo cluster galaxies but varies between 0^m00 and 0^m16 (Burstein & Heiles, 1984). These corrections, as listed in the RC3 and whose mean value is only 0^m05 , have been applied to all galaxies in Table 2 and 3.

If, instead, one assumes $A^0 = 0$ for the Virgo galaxies, the slope of the TF relation is not changed within the error limits; the dispersion becomes insignificantly smaller (Table 4, solution 8).

6.5. The effect of different input parameters

The solutions 1-8 in Table 4 (column 8) give an overview how the Virgo cluster modulus varies as different sources of the magnitudes, line widths, and internal absorptions are used. Also shown is the effect of increasing the sample of spirals with $i > 45^\circ$ by those with $30^\circ < i < 45^\circ$ and by replacing the optically selected fiducial sample by the members within the X-ray contour. Finally in solution 8 the small effect of assuming zero Galactic absorption for the cluster members is shown.

The resulting Virgo cluster moduli in column 8 span a range of 31^m48 to 32^m00 . There is no objective way to discriminate between the different solutions. We therefore take a straight mean over the solutions 1-7 and obtain

$$(m - M)_{\text{Virgo}} = 31^m65 \pm 0^m07. \quad (9)$$

7. Testing the internal consistency of the results

Several tests are performed to check the internal consistency of the derived TF distances. Without loss of generality we consider here only the TF distances of solution 1 in Table 4.

The individual distance moduli are shown in Fig. 6 as a function of redshift. There is no significant correlation between the TF distance and the recession velocity. From Fig. 6 one could argue that the five galaxies with redshifts larger than the gap at $v_{\text{LG}} \sim 1700 \text{ km s}^{-1}$ do not belong to the cluster. However, the gap is a fluke of small sample statistics, because it does not appear in

the velocity distribution of *all* Virgo members (Binggeli et al. 1993). Moreover the high-velocity galaxies have closely the same mean TF distance as the rest of the fiducial sample. There is no objective argument to exclude any galaxy in Fig. 6 from cluster membership. The only statistically significant effect is the dichotomy between subclusters A and B as discussed in Sect. 5.1.

Figure 7 shows the individual TF distances plotted against inclination. Any systematic error of the inclinations affects both the corrected line widths and the corrections for internal absorption and translates into a dependency of the TF distances on inclination. However, no such trend exists, not even for the spirals with $30^\circ < i < 45^\circ$.

Similarly we do not find a dependence of the TF distances on the Hubble type (Fig. 8). This would have been the case if the corrections for internal absorptions, which are a function of the Hubble type, were systematically wrong or if the TF relation was significantly different for different Hubble types. (The question whether TF distances depend on Hubble type is largely determined by the internal-absorption correction used.)

As a next test we show a plot of the individual TF distances as a function of line width (Fig. 9). The obtained distances do not depend on the line width which must be the case if the slope of the TF relation has been determined correctly.

In Fig. 10 there is a trend of galaxies becoming fainter with increasing TF distances. This can most naturally be explained by the cluster depth effect. If the galaxies are randomly distributed in the cluster as to absolute magnitude M_B , then the nearer galaxies must be apparently brighter. A least square fit through the data gives $(m - M) = (0.12 \pm 0.06)m_B + 29^m95$. This implies that the cluster has an effective depth of $\pm 0^m4$ as outlined by the spirals of the five-magnitude interval $10^m < m_B < 15^m$.

The eight galaxies fainter than 14^m , which all seem to lie on the far side of groups A and B respectively, do not show an unusual behaviour in the correlation of the parameters in Figs. 6-9. Two of the eight galaxies, i.e. NGC 4353 and IC 3298, have particularly large TF distance moduli of $(m - M) \approx 32^m6$. In spite of this NGC 4353 must be assigned to the cluster with a recession velocity of only $v_{LG} = 982 \text{ km s}^{-1}$. It is therefore arbitrary to exclude any galaxy of the fiducial sample from cluster membership only on the basis of its large TF distance. Therefore, there is also no rational reason to exclude IC 3298 ($v_{LG} = 2355 \text{ km s}^{-1}$) from the cluster.

8. Systematic differences between calibrators and Virgo spirals

The Virgo cluster distance depends on the *assumption* that field and cluster galaxies obey the same TF relation. This assumption can now be tested with the complete *UBVRI* photometry of Schröder (1996). It turns out that the cluster galaxies are redder in $(B - I)$ (corrected for internal and Galactic reddening) at a given line width than the 18 calibrators which are predominantly field galaxies. This means that the TF relation cannot be the same for the two sets of galaxies *in all*

wavelengths. The cluster galaxies are also more HI-deficient than the calibrators. The hydrogen deficiency D_{HI} is here defined following YFO (1997), whereby the color residuals $\Delta(B - I)$ at fixed line width correlate well with D_{HI} . The dependency of the individual TF distances on $\Delta(B - I)$ and D_{HI} are shown by Schröder & Tammann (1996) for five different passbands. Tammann & Federspiel (1997) have argued that the best Virgo distance is obtained by averaging over all color and D_{HI} -corrected *UBVRI* moduli. The result is that the straight TF modulus in *B* is $0^{\text{m}}07 \pm 0^{\text{m}}02$ larger than the mean of all corrected moduli. We apply this correction to eq. (9) to obtain the finally adopted Virgo modulus of

$$(m - M)_{\text{Virgo}}^0 = 31^{\text{m}}58 \pm 0^{\text{m}}07 \quad (10)$$

where the error is taken from eq. (9).

It may be noted in passing that the TF modulus in *V* seems least sensitive to the cluster effect and that the *uncorrected* TF modulus in *I* is $0^{\text{m}}09$ too small (Schröder & Tammann 1996).

9. The three-dimensional structure of the Virgo cluster from TF data

Individual Tully-Fisher distances are reliable enough that they can be used to cautiously explore the three-dimensional structure of the Virgo cluster. Figure 11 shows a visualisation of the spatial distribution of the members of subgroups A and B as well as of the calibrators that belong to the Virgo cluster. All distances given in this section are based on Table 4, solution 1. The *x-y* plane is perpendicular to the line-of-sight from the Sun to M87, i.e. it is a tangent plane to the celestial sphere. The spherical coordinates were transformed into linear coordinates at the distance of the individual galaxies. Since the distance moduli obtained from the TF relation are a logarithmic measure, the *z* axis is logarithmic (log distance in Mpc). A typical error of an individual distance of the order of the scatter of the TF relation [$0^{\text{m}}6$ in $(m - M)$] corresponds to an uncertainty of 0.1 in *z* on the line of sight to M87.

The calibrators among the Virgo galaxies and NGC 4496A are shown as crosses at their respective *Cepheid* distance. Three of them (N4321, N4496A, and N4536) are among the dozen closest Virgo galaxies, whereas N4639 is on the far side of subcluster A. These four galaxies with known Cepheids provide a check on the accuracy of about $0^{\text{m}}45$ of the individual TF distances (cf. Table 5).

From the apparent angular size and the depths calculated from the TF distances (deconvolved with the intrinsic dispersion of about $0^{\text{m}}40$ of the TF relation) we derive a linear diameter-to-depth ratio for subcluster A of about 1:1.5.

Figure 12 emphasizes that subcluster B on average lies at a greater distance than subcluster A ($0^{\text{m}}46 \pm 0^{\text{m}}18$ in the distance modulus). B appears rather elongated in depth although it is quite compact in the projection on the celestial sphere. The diameter-to-depth ratio for B is about 1:5. The ratios may be somewhat smaller if we have underestimated the distance errors.

10. Discussion

The error of the adopted TF modulus of the Virgo cluster in eq. (10) reflects only the random error. Systematic error sources are listed in Table 6.

Remarks to Table 6 are as follows. The zeropoint error of the P-L relation has been discussed in Sect. 2.1. Forcing extreme slopes of -7.50 and -6.50 on the TF relation of the fiducial sample and the calibrating galaxies changes the distance modulus by $\pm 0^m10$. Different precepts of weighting the data of the calibrators and Virgo spirals can influence the modulus by 0^m08 . Giving higher weight to the X-ray sample or omitting it altogether could change the adopted distance modulus by 0^m1 at most. Taking the input B magnitudes and/or line widths w from different sources has essentially no effect on the Virgo distance (Sects. 6.1. and 6.2.); but different precepts of the internal-absorption correction affect the modulus by $\pm 0^m10$ (Table 4, solutions 1-3 versus 5-7). Different properties of the calibrators and the cluster galaxies have been accounted for by excluding the truncated cluster galaxies and by applying a mean correction for differences in $(B - I)$ and D_{HI} (Sect. 8); the remaining maximum error is estimated to be $\pm 0^m05$. The calibrators are systematically *less* inclined ($\langle i \rangle = 55^\circ$) than the cluster galaxies ($\langle i \rangle = 72^\circ$). Consequently the mean RC3 correction for internal absorption is $\langle A^i \rangle = 0^m34$ for the former and $\langle A^i \rangle = 0^m66$ for the latter. Yet the two samples become more similar if the fiducial sample is increased by the cluster galaxies with $30^\circ < i < 45^\circ$. In that case the cluster sample has $\langle i \rangle = 62^\circ$ and $\langle A^i \rangle = 0^m45$ without changing the cluster modulus by more than 0^m03 (Table 4, solutions 3 and 7). Moreover the individual TF distances are independent of inclination (Fig. 7), which would not be the case if the internal absorption corrections were inadequate. The conclusion is that the internal absorption corrections introduce a systematic error of not more than 0^m05 .

Summing the errors in quadrature in Table 6 gives an external error of $\pm 0^m23$. Adding this in quadrature to the internal error in eq. (10) gives the final distance modulus of the Virgo cluster (A and B) to be

$$(m - M)_{\text{Virgo}}^0 = 31^m58 \pm 0^m24 \text{ (external error)} \quad (11)$$

or $r_{\text{Virgo}} = 20.7 \pm 2.4$ Mpc.

The decisive element of the present distance determination of the Virgo cluster is that a *complete* sample has been used. It is fortunate that low-luminosity spirals *do not exist*, and that the Virgo Cluster Catalog (VCC; Binggeli et al. 1985) goes much fainter than the faintest spirals. The faintest galaxies in that catalog are of morphological types Im and dE, well fainter than the absolute magnitude limit of the TF calibrators of Table 2 and Fig. 2. The sample studied here is therefore indeed *complete* for spirals. The importance of completeness is illustrated in Fig. 13, where the fiducial sample is cut by different magnitude cutoffs. The brighter the cutoff is the smaller is the distance modulus even for *complete* flux-limited samples (cf. Teerikorpi 1987).

Giovanelli et al. (1997a, b) have given TF data for inclined spirals in 24 clusters. There are 23 galaxies per cluster on average which reach $\sim 3^m8$ into the luminosity function on average.

This would be barely sufficient to derive an unbiased distance from a complete sample (Fig. 13). However, the cluster samples are admittedly *incomplete* at all levels but particularly at the fainter magnitudes. The authors derive excellent *relative* cluster distances as seen in Fig. 14 below, due to a very careful modelling of the cluster incompleteness. They have also attempted to obtain an absolute calibration by fitting the cluster data to the local distance-limited calibrators and suggest $H_0 = 69 \pm 5$ (Giovanelli et al. 1997c). Clearly this latter step is much more sensitive to the bias model than the relative distances. If the authors had used the Virgo cluster distance of eq. (11) they would have obtained from their cluster data $H_0 = 57$ as below in eq. (15). Vice versa their value of $H_0 = 69$ would require $(m - M)_{\text{Virgo}} = 31^{\text{m}}17$ which we deem to be highly improbable.

In a recent application of the TF method to the Virgo cluster YFO (1997) have analyzed a less restrictive sample of 108 inclined Virgo spirals and irregulars. Their mean distance is $(m - M) = 31^{\text{m}}81$ with a large scatter of $\sigma_{(m-M)} = 0^{\text{m}}93$. Restricting the sample to the 63 galaxies with $\delta > 10.5^\circ$ – which roughly corresponds to subcluster A – yields $(m - M) = 31^{\text{m}}62$ with $\sigma_{(m-M)} = 1^{\text{m}}00$. These moduli are somewhat larger than those of the fiducial sample and subcluster A, respectively, from above. The scatter of the latter solutions is significantly less. Moreover YFO did not correct the line widths for turbulence, resulting in a quite steep TF relation which leads to a significant dependence of the individual distances on the corrected line widths. The extremely low cluster modulus of $(m - M) = 31^{\text{m}}09$ finally adopted by YFO for the M87 subcluster was achieved by confining their sample to only galaxies with $\delta > 10.5^\circ$ and by excluding 21 spirals with $(m - M) > 32^{\text{m}}0$. We take exception to these *artificial* cuts which prevent any objective distance determination of the Virgo cluster. There is no objective reason to exclude the more distant galaxies which clearly are members. They not only perfectly fit under the distance distribution curve (cf. Fig. 12) but also are indistinguishable from other cluster members on the basis of both their positions within the optical and X-ray contour of the cluster in the sky and also their velocities.

Shanks (1997), using both Cepheid and SNIa distances as calibrators of the TF relation, has obtained an internally consistent zeropoint correction of $+0^{\text{m}}46 \pm 0^{\text{m}}11$ to the TF distance of the Virgo cluster by Pierce & Tully (1988), obtaining now $(m - M)_{\text{Virgo}} = 31^{\text{m}}43 \pm 0^{\text{m}}20$. Since the Pierce & Tully sample is *incomplete* even this corrected distance must suffer the Teerikorpi incompleteness bias and be systematically too low (Fig. 13).

The Virgo modulus in eq. (11) is identical within the errors with the result of five independent methods, including Cepheids, SNeIa, globular clusters, novae, and the $D_n - \sigma$ method, giving $31^{\text{m}}66 \pm 0^{\text{m}}08$ (Sandage & Tammann 1997).

11. Conclusion

11.1. H_0 from the observed, infall-corrected velocity

The Virgo cluster has been used frequently as a cosmic milestone to derive the Hubble constant from its velocity and its distance. The observed mean *heliocentric* velocity of the cluster is $v = 1050 \pm 35 \text{ km s}^{-1}$ (Binggeli et al. 1993) or $v_{\text{LG}} = 922 \text{ km s}^{-1}$. This latter value must be transformed to the cosmic recession velocity that takes the Virgocentric infall of the Local Group into account. For the Virgocentric infall we adopt the value of $v_{\text{infall}} = 220 \pm 50 \text{ km s}^{-1}$ (Tammann & Sandage 1985), which is in excellent agreement with $v_{\text{infall}} = 224 \pm 90 \text{ km s}^{-1}$ (Bureau et al. 1996) and in statistical agreement with $v_{\text{infall}} = 275 \pm 90 \text{ km s}^{-1}$ of Hamuy et al. (1996); it is further supported in Sect. 11.2. Thus the infall-corrected recession velocity of the Virgo cluster is $1142 \pm 61 \text{ km s}^{-1}$. This combined with the adopted distance of the Virgo cluster (eq. 11) gives a local Hubble constant of

$$H_0 = 55 \pm 7 \text{ km s}^{-1} \text{ Mpc}^{-1}. \quad (12)$$

Although the just described route to H_0 is quite common, it is surpassed by the calibration of the Hubble diagram of clusters addressed in the next section, which ties the Virgo cluster to distant clusters and leads to a value of the Hubble constant that is valid over a much larger volume.

As an exercise we consider also the effect on H_0 if the subclusters A and B are reduced separately. The data are set out in Table 7. The mean velocity of the two aggregates corrected for an infall velocity of 220 km s^{-1} is taken from Binggeli et al. (1993). The distance moduli are calculated from solutions 1-3 and 5-7 in Table 4, but now separately for A and B. Here the X-ray sample is, by necessity, not considered. The weighted mean of $H_0 = 56 \pm 3$ reflects only the internal error (cf. Sect. 10).

11.2. H_0 from the Hubble diagram of galaxy clusters

Cluster distances relative to the Virgo cluster are available for 17 clusters from various methods such as the Tully-Fisher (TF) method, the $D_n - \sigma$ relation, and first-ranked cluster galaxies (for a compilation see Jerjen & Tammann 1993). In addition, high weight *relative* TF distances are available for 24 clusters from Giovanelli (1996). The latter list does not include the Virgo cluster, but since eight clusters are in common, the two lists can be merged with a mean error of only 0.05 mag. The double cluster A 2634/66 is not used here because Giovanelli (1996) only gives a distance for A 2634. The resulting Hubble diagram (Fig. 14) contains 31 clusters with distances relative to the Virgo cluster (cf. also Table 1 of Tammann & Federspiel 1997).

Clusters with $v_0 < 3000 \text{ km s}^{-1}$ are corrected for a Virgocentric infall model with a local infall velocity of 220 km s^{-1} . More distant clusters do not partake of the local motion with respect to the CMB. They are therefore corrected for a CMB vector of 630 km s^{-1} . The dividing limit of 3000 km s^{-1} is derived elsewhere (cf. Jerjen & Tammann 1993; Federspiel, Sandage, & Tammann

1994, Figs. 17-19; Giovanelli 1996); the exact choice has no effect on the following conclusions.

The ridge line in Fig. 14 is represented by

$$\log v^{\text{CMB}} = 0.2 \left[(m - M) - (m - M)_{\text{Virgo}} \right] + (3.070 \pm 0.011). \quad (13)$$

The slope of 0.2 is forced, the strongly deviating Eridanus cluster is omitted.

Simple transformation of eq. (13) gives

$$\log H_0 = \log v^{\text{CMB}} - \log r_{\text{Mpc}} = -0.2(m - M)_{\text{Virgo}} + (8.070 \pm 0.011) \quad (14)$$

Inserting the distance modulus of the Virgo cluster from eq. (11) into eq. (14) gives the value of H_0 for distances as large as $11\,000 \text{ km s}^{-1}$:

$$H_0 = 57 \pm 7 \text{ km s}^{-1} \text{ Mpc}^{-1}. \quad (15)$$

Note that reading eq. (13) at *zero relative distance* also predicts the velocity of the Virgo cluster itself in the CMB frame $v_{\text{Virgo}}^{\text{CMB}} = 1175 \pm 30 \text{ km s}^{-1}$. This is the velocity one would observe in the absence of all local peculiar or streaming velocities. Comparing this value with the actually observed cluster velocity of $v_{\text{LG}} = 922 \pm 35 \text{ km s}^{-1}$, one obtains a Virgocentric infall velocity of the Local Group of $v_{\text{infall}} = 253 \pm 46 \text{ km s}^{-1}$ (cf. Jerjen & Tammann 1993). We take this as a confirmation of $v_{\text{infall}} = 220 \pm 50 \text{ km s}^{-1}$ adopted in Sect. 11.1.

It must be stressed that the determination of H_0 from eq. (14) depends only on the quality of the Virgo cluster distance and on the relative distances to other clusters, but it is totally independent of any observed or inferred velocity of that cluster (Sandage & Tammann 1996).

11.3. Comparison with external values of H_0

Several authors have suggested to derive H_0 at the position of the Coma cluster (e.g. Baum et al. 1995, 1996; Thomsen et al. 1997; Hjorth & Tanvir 1997). The result is typically $H_0 \approx 70$. However, the experiment with only a single cluster is much more difficult than the route via the Virgo cluster tied to the expansion field of *many* clusters (Fig. 14). The reason is, first, that comparable objects in Coma are almost four magnitudes fainter than in Virgo, and, secondly, that the velocity of Coma in the CMB frame is quite poorly known. The observed mean velocity is $v_{\text{LG}} = 6912 \text{ km s}^{-1}$ (Zabludoff et al. 1993). It is generally *assumed* that the cluster does not take part of the local motion relative to the CMB frame. In that case $v_{\text{Coma}}^{\text{CMB}} = 7194 \text{ km s}^{-1}$. However, clusters have random motions (in the radial direction) of typically 450 km s^{-1} (Jerjen & Tammann 1993), and Coma deviates indeed strongly from the Hubble line in Fig. 14. If a modulus difference between Coma and Virgo of $\Delta(m - M)_{\text{Coma-Virgo}} = 3^{\text{m}}72$ is adopted (Dekel 1996) eq. (13) gives $v_{\text{Coma}}^{\text{CMB}} = 6500 \text{ km s}^{-1}$. Hence the velocity uncertainty alone affects the result of H_0 by $\sim 10\%$.

The most direct way to derive the Hubble constant is through the Hubble diagram of supernovae of type Ia (SNe Ia) which is by now calibrated by seven SNe Ia with known Cepheid distances. The result of $H_0 = 58 \pm 8$ (external error)(Saha et al. 1997) is in agreement with the present result. The only interdependence of these determinations of H_0 is that two Cepheid distances used to calibrate the SNe Ia are also used in Table 2 to calibrate the TF relation.

Luminosity class distances and TF distances of field galaxies give equally consistent values of the Hubble constant, after correction of the Malmquist bias, of $H_0 = 55 \pm 5$ (Sandage & Tammann 1975; Sandage 1996a,b and references therein; Theureau et al. 1997).

The conclusion is that the three independent routes through (1) the Virgo cluster, (2) SNe Ia, and (3) field galaxies all give $H_0 = 55 \pm 5$ km s⁻¹ Mpc⁻¹.

An independent way to determine extragalactic distances comes from a physical understanding of the objects considered without the necessity to use astronomical luminosity (or size) calibrators. The purely physical calibration of the P-L relation of Cepheids has already been mentioned (Sect. 2.1). For several X-ray clusters Sunyaev-Zel'dovich distances have become available. Three papers having appeared during the last months give an (unweighted) mean of $H_0 = 58 \pm 15$ (Holzapfel et al. 1997; Lasenby & Jones 1997; Myers et al. 1997). Rephaeli & Yankovitch (1997) have pointed out that the inclusion of relativistic effects reduces this value by ~ 10 units. Recent H_0 determinations from variable, gravitationally lensed quasars give $H_0 = 59 \pm 15$ (Keeton & Kochanek 1997; Kundić et al. 1997; Falco et al. 1997; Schechter et al. 1997). The first interpretations of the CMB fluctuation spectrum suggest even lower values (Lasenby & Jones 1997; Lineweaver 1997).

In the light of this evidence values of H_0 below 45 and above 65 become improbable.

We have made use of the Lyon-Meudon Extragalactic Database (LEDA) supplied by the LEDA team at the CRAL Observatoire de Lyon (France). We thank S.M.G. Hughes for his results prior to publication and H. Böhringer for the Virgo X-ray image from the ROSAT all-sky survey. We are indebted to M. Bershadsky for lending us his BCES software. We thank the Referee for valuable comments. MF and GAT gratefully acknowledge the support of the Swiss National Science Foundation. AS acknowledges support from NASA through the Space Telescope Science Institute in the SNe Ia calibration project using HST.

REFERENCES

- Aaronson, M., Huchra, J., & Mould, J. 1979, ApJ, 229, 1
Akritas, M.G., Bershadsky, M.A., & Bird, C.M. 1996, ApJ, 470, 706
Arsenault, R., Boulesteix, J., Georgelin, Y., & Roy, J.-R. 1988, A&A, 200, 29
Baum, W., et al. 1995, AJ, 110, 2537

- Baum, W., et al. 1996, BAAS, 189, 12.04
- Beaulieu, J.P., & Sasselov, D.D. 1996 1997, A&A, 318, 47 (astro-ph 9612217)
- Binggeli, B., Popescu, C.C., & Tammann, G.A. 1993, A&AS, 98, 275
- Binggeli, B., Sandage, A., & Tammann, G.A. 1985, AJ, 90, 1681
- Böhm-Vitense, E. 1997, AJ, 113, 13
- Böhringer, H., Briel, U.G., Schwarz, R.A., Voges, W., Hartner, G., & Trümper, J. 1994, Nature, 368, 828
- Bosma, A., Goss, W.M., & Allen, R.J. 1981, A&A, 93, 106
- Bureau, M., Mould, J.R., & Staveley-Smith, L. 1996, ApJ, 463, 60
- Burstein, D., & Heiles, C. 1984, ApJS, 54, 33
- Chiosi, C., Wood, P., & Capitanio, N. 1993, ApJS, 86, 541
- Comte, G., Monnet, G., & Rosado, M. 1979, A&A, 72, 73
- Dekel, A. 1996, private communication
- de Vaucouleurs, G., de Vaucouleurs, A., Corwin, H.G., Buta, R.J., Paturel, G., & Fouqué, P. 1991, Third Reference Catalogue of Bright Galaxies (RC3) (New York: Springer)
- Di Benedetto, G.P. 1997, ApJ, in press
- Faber, S.M., Wegner, G., Burstein, D., Davies, R.L., Dressler, A., Lynden-Bell, D., & Terlevich, R.J. 1989, ApJS, 69, 763
- Falco, E.E., Lehár, J., & Shapiro, I.I. 1997, AJ, in press
- Feast, M. 1995, in *Astrophys. Applications of Stellar Pulsations*, ASP Conf. Series, 83, p. 209
- Feast, M.W., & Catchpole, R.M. 1997, MNRAS, 286, L1
- Feast, M.W., & Walker, A.R. 1987, ARA&A, 25, 345
- Federspiel, M., Sandage, A., & Tammann, G.A. 1994, ApJ, 430, 29
- Ferrarese, L., et al. 1996, ApJ, 464, 568
- Fouqué, P., Bottinelli, L., Gouguenheim, L., & Paturel, G. 1990, ApJ, 349, 1
- Freedman, W.L., & Madore, B. 1994, ApJ, 427, 628
- Giovanelli, R. 1996, private communication
- Giovanelli, R., Haynes, M.P., Salzer, J.J., Wegner, G., da Costa, L.N., & Freundling, W. 1994, AJ, 107, 2036
- Giovanelli, R., et al. 1997a, AJ, 113, 22
- Giovanelli, R., et al. 1997b, AJ, 113, 53
- Giovanelli, R., Haynes, M.P., da Costa, L.N., Freundling, W., Salzer, J.J., & Wegner, G. 1997c, ApJ, 477, L1

- Gouguenheim, L. 1969, A&A, 3, 281
- Graham, J.A., et al. 1996, BAAS, 188, 12.14
- Grosbøl, P.J. 1985, A&AS, 60, 261
- Guhathakurta, P., van Gorkum, J.H., Kotanyi, C.G., & Balkowski, C. 1988, AJ, 96, 851
- Hamuy, M., Phillips, M.M., Suntzeff, N.B., Schommer, R.A., Maza, J., & Avilés, R. 1996, AJ, 112, 2398
- Hill, R.J., et al. 1997, ApJS, in press
- Hjorth, J., & Tanvir, N.R. 1997, ApJ, in press (astro-ph 9701025)
- Hoffman, G.L., Helou, G., Salpeter, E.E., Glosson, J., & Sandage, A., 1987, ApJS, 63, 247
- Hoffman, G.L., Lewis, B.M., Helou, G., Salpeter, E.E., & Williams, H.L., 1989, ApJS, 69, 65
- Holzappel, W.L., et al. 1997, ApJ, 480, 449
- Huchtmeier, W.K., & Richter, O.-G. 1988, A&A, 203, 237
- Huchtmeier, W.K., & Richter, O.-G. 1989, A&A, 210, 1
- Hughes, S.M.G. 1996, private communication
- Jerjen, H., & Tammann, G.A. 1993, A&A, 276, 1
- Keeton, C.R., & Kochanek, C.S. 1997, preprint
- Kelson, D.D. et al. 1996, ApJ, 463, 26
- Kochanek, C.S. 1997, preprint (astro-ph 9703059)
- Kraan-Korteweg, R.C., Cameron, L.M., & Tammann, G.A. 1988, ApJ, 331, 620
- Kundić, T., Cohen, J.G., Blanford, R.D., & Lubin, L.M. 1997, preprint (astro-ph 9704109)
- Laney, C.D., & Stobie, R.S. 1992, in *Variable Stars and Galaxies*, ed. B. Warner, ASP Conf. Series, 30, p. 119
- Lasenby, A.N., & Jones, M.E. 1997, in *The Extragalactic Distance Scale*, eds. M. Livio, M. Donahue, & N. Panagia, Baltimore: STScI, p. 76
- Lee, M.G., Freedman, W.L., & Madore, B.F. 1993, ApJ, 417, 553
- Lineweaver, C.H. 1997, preprint (astro-ph 9702042)
- Macri, L. 1996, in *The Extragalactic Distance Scale*, poster papers from the STScI Symposium, May 1996, eds. M. Livio, M. Donahue, & N. Panagia
- Madore, B., & Freedman, W.L. 1991, PASP, 103, 933
- Madore, B., & Freedman, W.L. 1997, ApJLetters, in press
- Myers, S.T., Baker, J.E., Readhead, A.C.S., Leitch, E.M., & Herbig, T. 1997, ApJ, preprint (astro-ph 9703123)
- Öpik, E. 1921, Mirovedenie, 10, 12

- Öpik, E. 1922, ApJ, 55, 406
- Panagia, N., et al. 1996, Poster papers from the STScI, p. 54
- Pierce, M.J. 1994, ApJ, 430, 53
- Pierce, M.J., & Tully, R.B. 1988, ApJ, 330, 579
- Rephaeli, Y., & Yankovitch, D. 1997, ApJ, 481, L55
- Rogstad, D.M., & Shostak, G.S. 1972, ApJ, 176, 315
- Saha, A., & Labhardt, L. 1997, private communication
- Saha, A., Sandage, A., Labhardt, L., Tammann, G.A., Macchetto, F.D., & Panagia, N. 1996a, ApJS, 107, 693
- Saha, A., Sandage, A., Labhardt, L., Tammann, G.A., Macchetto, F.D., & Panagia, N. 1996b, ApJ, 466, 55
- Saha, A., Sandage, A., Labhardt, L., Tammann, G.A., Macchetto, F.D., & Panagia, N. 1997, ApJ, preprint
- Saio, H., & Gautschy, A. 1997, in press
- Sakai, S., et al. 1996, BAAS, 189, 12.06
- Sandage, A. 1988, PASP, 100, 935
- Sandage, A. 1993, AJ, 106, 703
- Sandage, A. 1996a, AJ, 111, 1
- Sandage, A. 1996b, AJ, 111, 18
- Sandage, A. 1996c, BAAS, 28, No. 1, 52
- Sandage, A., Saha, A., Tammann, G.A., Labhardt, L., Panagia, N., & Macchetto, F.D. 1996, ApJ, 460, L15
- Sandage, A., & Tammann, G.A. 1971, ApJ, 167, 293
- Sandage, A., & Tammann, G.A. 1975, ApJ, 197, 265
- Sandage, A., & Tammann, G.A. 1976, ApJ, 210, 7
- Sandage, A., & Tammann, G.A. 1987, A Revised Shapley-Ames Catalog of Bright Galaxies (RSA), Carnegie Institution of Washington Publication 635
- Sandage, A., & Tammann, G.A. 1996, ApJ, 464, L51
- Sandage, A., & Tammann, G.A. 1997, in *Critical Dialogue on Cosmology Conference*, ed. N. Turok, Princeton, in press
- Sandage, A., Tammann, G.A., & Federspiel, M. 1995, ApJ, 452, 1
- Sasselov, D.D. et al. 1997, A&A, in press
- Schechter, P.L., et al. 1997, preprint

- Schröder, A. 1996, PhD thesis, University of Basel
- Schröder, A., & Tammann 1996, in *The Extragalactic Distance Scale*, poster papers from the STScI Symposium, May 1996, eds. M. Livio, M. Donahue, & N. Panagia, p. 63
- Seares, F.H. 1944, ApJ, 100, 255
- Sekiguchi, M., & Fukugita, M. 1997, preprint
- Shanks, T. 1997, preprint
- Silbermann, N.A., et al. 1996a, ApJ, 470, 1
- Silbermann, N.A. et al. 1996b, in *The Extragalactic Distance Scale*, poster papers from the STScI Symposium, May 1996, eds. M. Livio, M. Donahue, & N. Panagia, p. 67
- Sodemann, M., & Thomson, B. 1997, A&A, in press
- Stothers, R.B. 1988, ApJ, 329, 712
- Tammann, G.A. 1996, in *Reviews in Modern Astronomy 9*, ed. R.E. Schielicke, Hamburg: Astronomische Gesellschaft, p. 139
- Tammann, G.A., & Federspiel, M. 1997, in *The Extragalactic Distance Scale*, eds. M. Livio, M. Donahue, & N. Panagia, Cambridge University Press, in press
- Tammann, G.A., & Sandage, A. 1985, ApJ, 294, 81
- Tanvir, N.R. 1997, in *The Extragalactic Distance Scale*, eds. M. Livio, M. Donahue, & N. Panagia, Cambridge University Press, in press
- Tanvir, N.R., Shanks, T., Ferguson, H.C., & Robinson, D.R.T., 1995, Nature, 377, 27
- Teerikorpi, P. 1984, A&A, 141, 407
- Teerikorpi, P. 1987, A&A, 173, 39
- Teerikorpi, P. 1990, A&A, 234, 1
- Teerikorpi, P. 1993, A&A, 280, 443
- Theureau, G., et al. 1997, A&A, 322, 730
- Thomsen, B., Baum, W.A., Hammergren, M., & Worthey, G. 1997, ApJ, in press
- Tully, R.B., & Fisher, J.R. 1977, A&A, 54, 661
- van Leeuwen, F., Feast, M.W., Whitelock, P.A., & Yudin, B. 1997, MNRAS, in press
- Walker, A.R. 1993, in *New Perspectives on Stellar Pulsations and Pulsating Variable Stars*, eds. J.M. Nemec & J.M. Matthews, IAU Coll. 139, p. 15
- Warmels, R.H. 1988, A&AS, 72, 19
- Yasuda, N., Fukugita, M., & Okamura, S. 1997, ApJS, 108, 417 (YFO)
- Zabludoff, A., Geller, M., Huchra, J., & Vogeley, M. 1993, AJ, 106, 1273

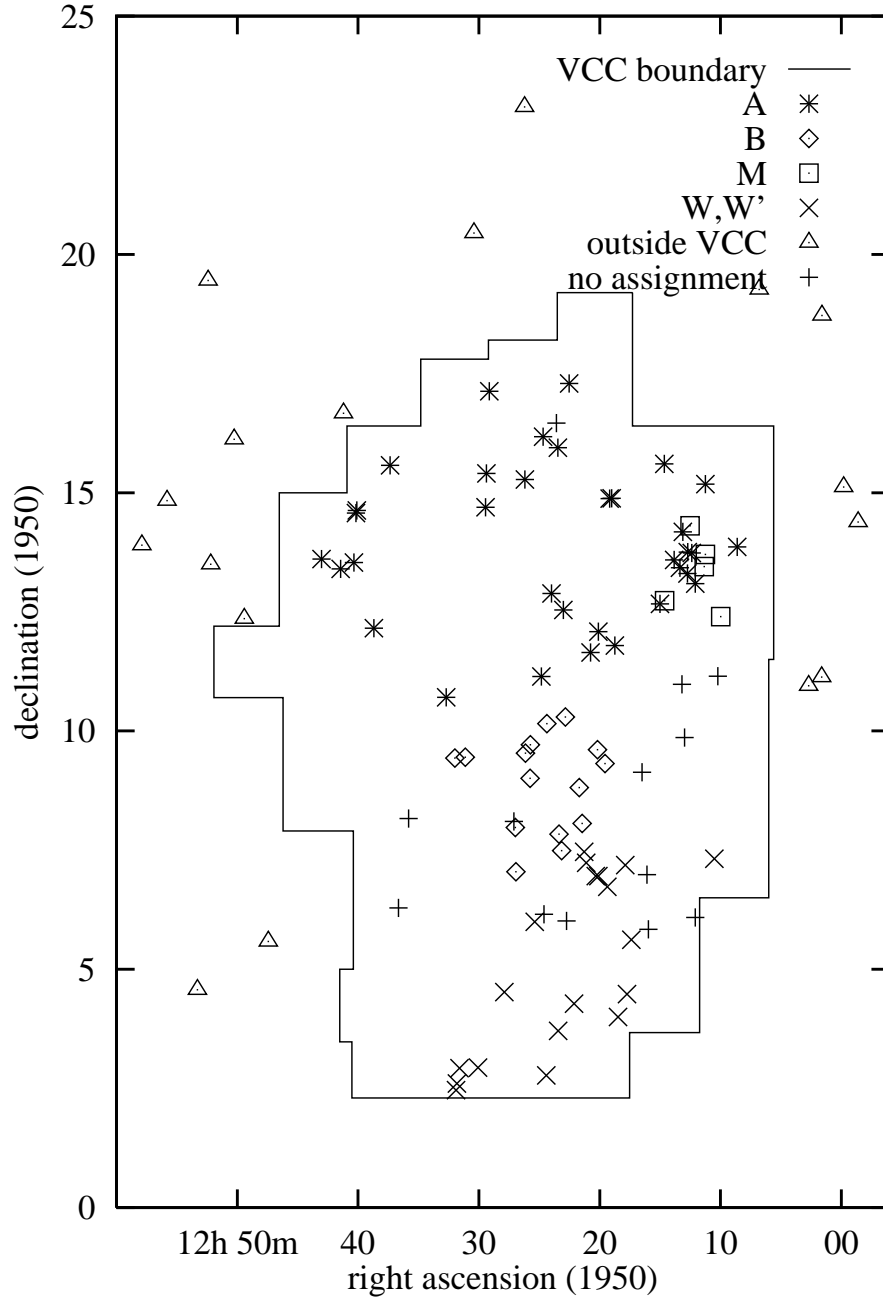


Fig. 1.— Positions of the non-peculiar spirals of Table 3 with $i > 45^\circ$ in the sky. The symbols denote the membership to a Virgo cluster subgroup assigned by Binggeli et al. (1993). Also shown is the boundary of the VCC field (Binggeli et al. 1985).

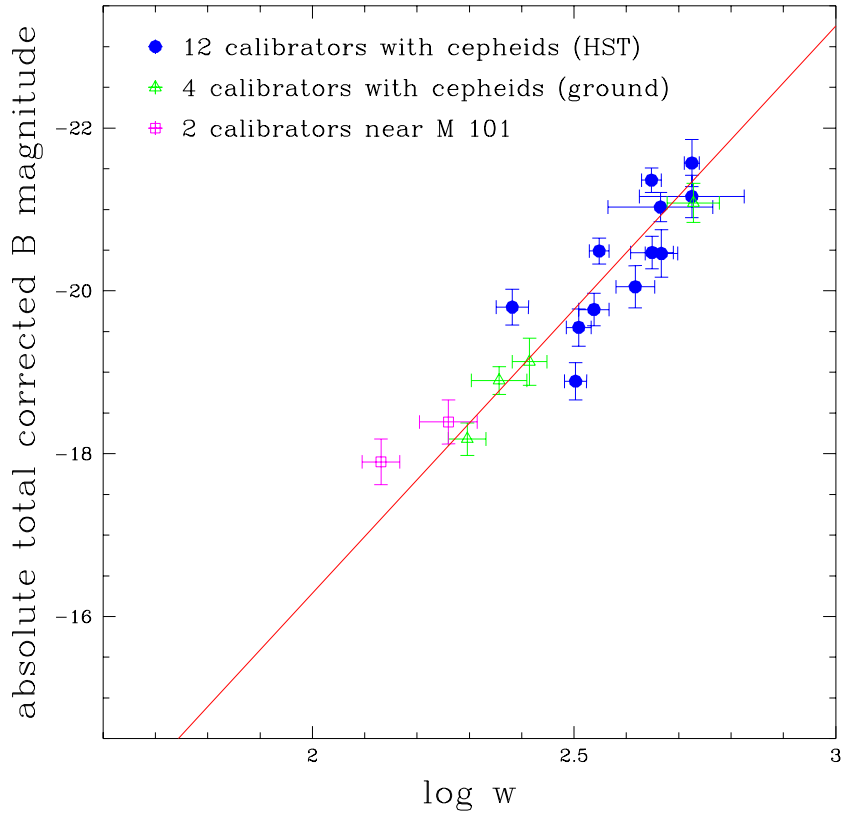


Fig. 2.— Tully-Fisher relation for the calibrators of Table 2. Twelve calibrators have Cepheid distances determined with HST, 4 have ground-based Cepheid distances, 2 are members of the relatively tight M101 group without individual Cepheid distances. The error bars show the total errors in absolute magnitude and log linewidth which were used as weights for the regression. The line represents the adopted calibration of eq. (3).

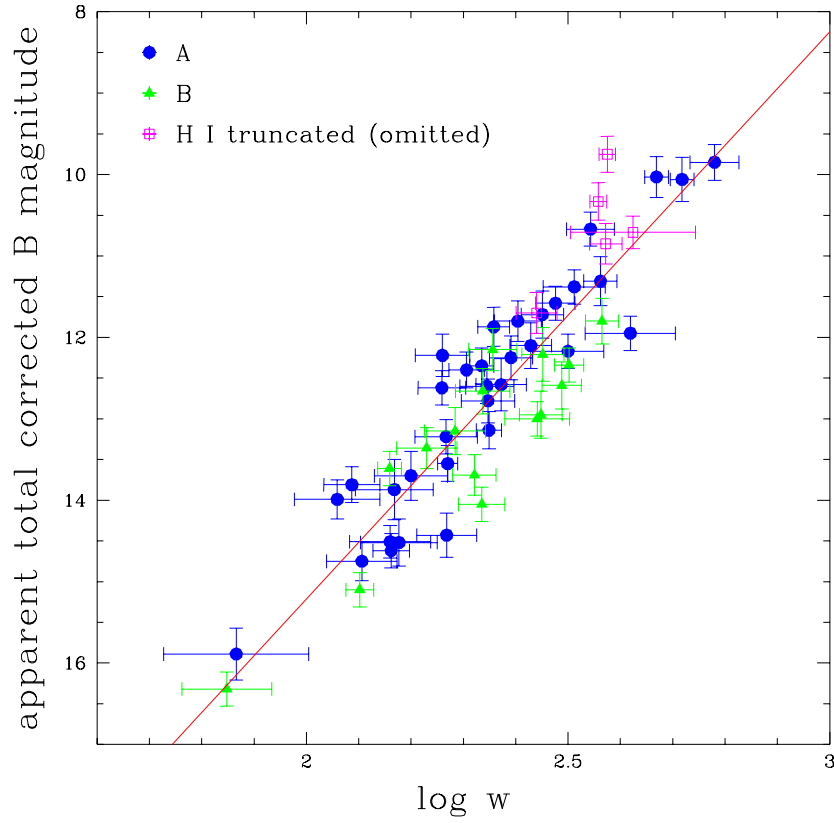


Fig. 3.— Tully-Fisher relation for the “fiducial Virgo sample”. The error bars show the individual total errors in magnitude and log linewidth which served as weights for the calculation of the regression line [eq.(3)]. Four galaxies with H I-truncated disks are also shown; they are systematically too bright for their line width and were excluded from the Tully-Fisher analysis.

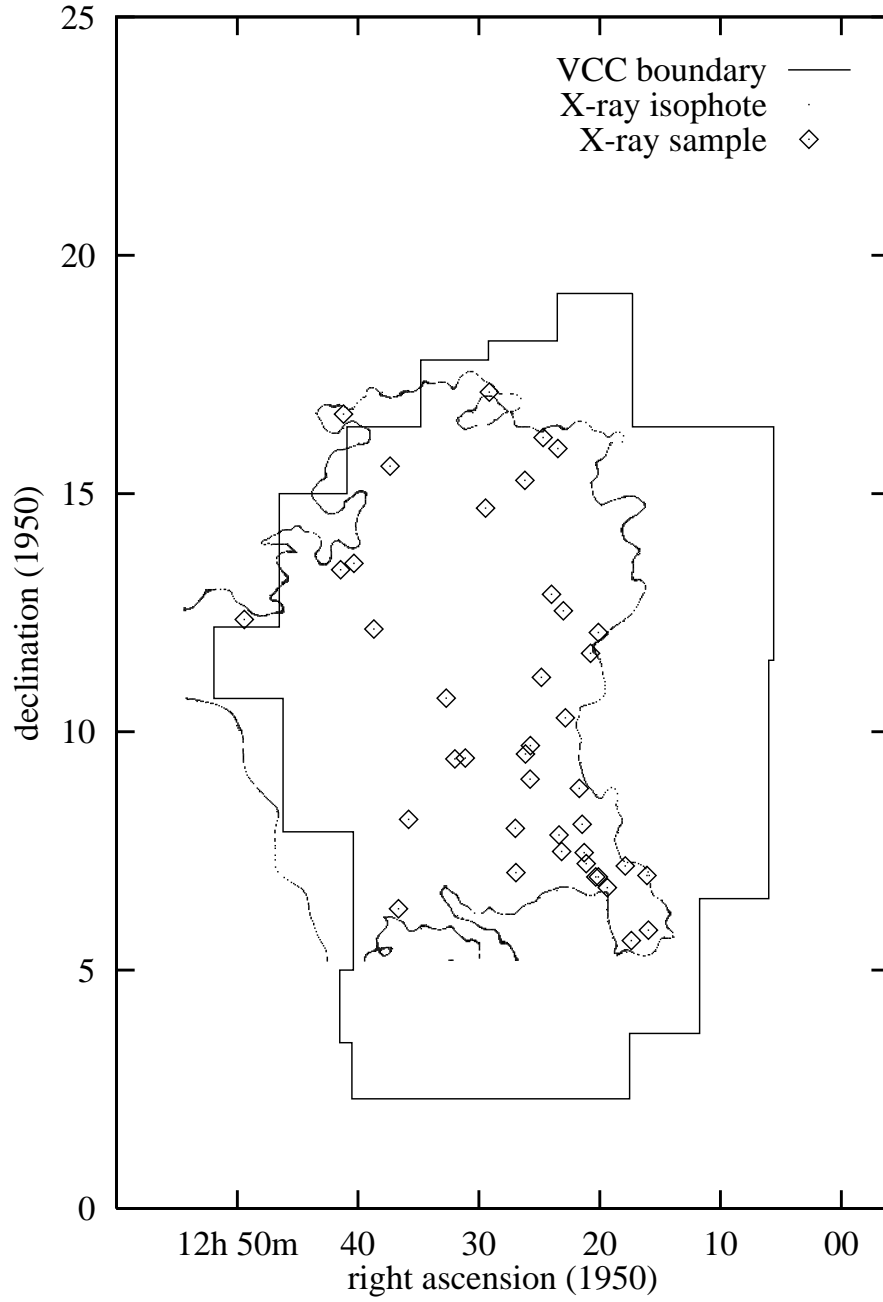


Fig. 4.— Positions of the members of the X-ray sample (flag X in Table 3, $i > 45^\circ$) and its defining isophote from ROSAT data. Also shown is the boundary of the VCC field (Binggeli et al. 1985).

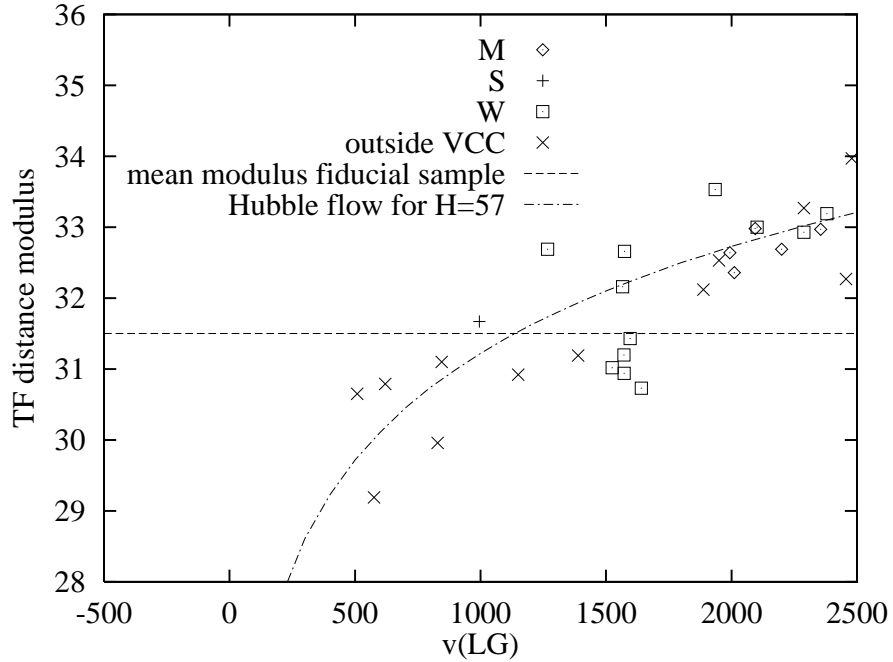


Fig. 5.— Tully-Fisher distances of all galaxies in Table 3 outside the fiducial sample and outside the X-ray sample as a function of redshift [referred to the centroid of the Local Group using eq. (3)]. Memberships of different subgroups are denoted by different symbols. There is a clear trend: the average distance is increasing with increasing redshift. This behaviour is compatible with a free Hubble expansion (the dash-dotted line shows the cosmic expansion assuming $H_0 = 57$). The conclusion is that these galaxies do not belong to the inner part of the Virgo cluster where internal motions dominate the redshifts.

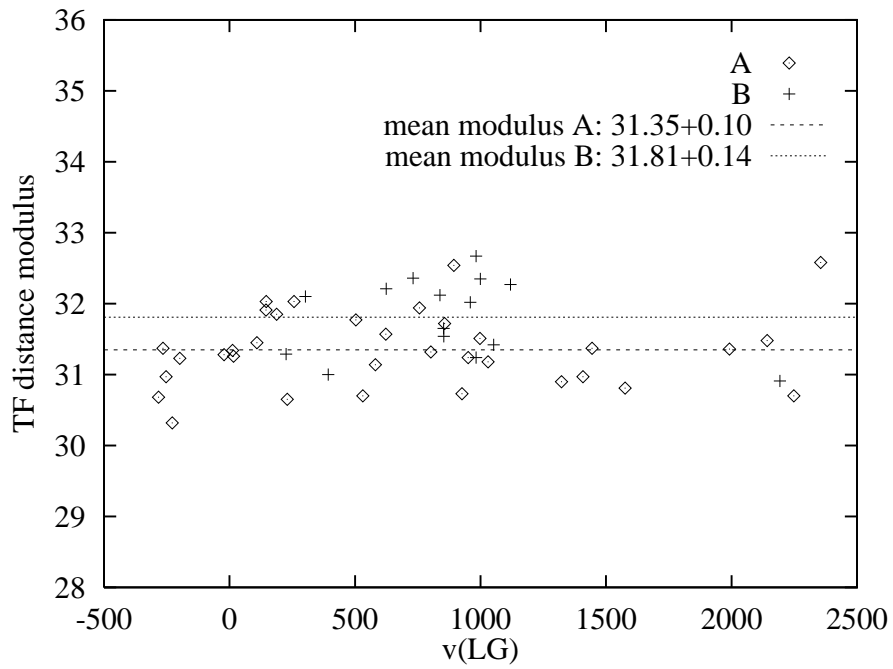


Fig. 6.— Tully-Fisher distances for the members of the “fiducial sample” as a function of redshift (referred to the centroid of the Local Group) using eq. (3). On average, subgroup B lies about $0^{\text{m}}46$ more distant than subgroup A. Obviously, the TF distances of the cluster galaxies do not depend on redshift.

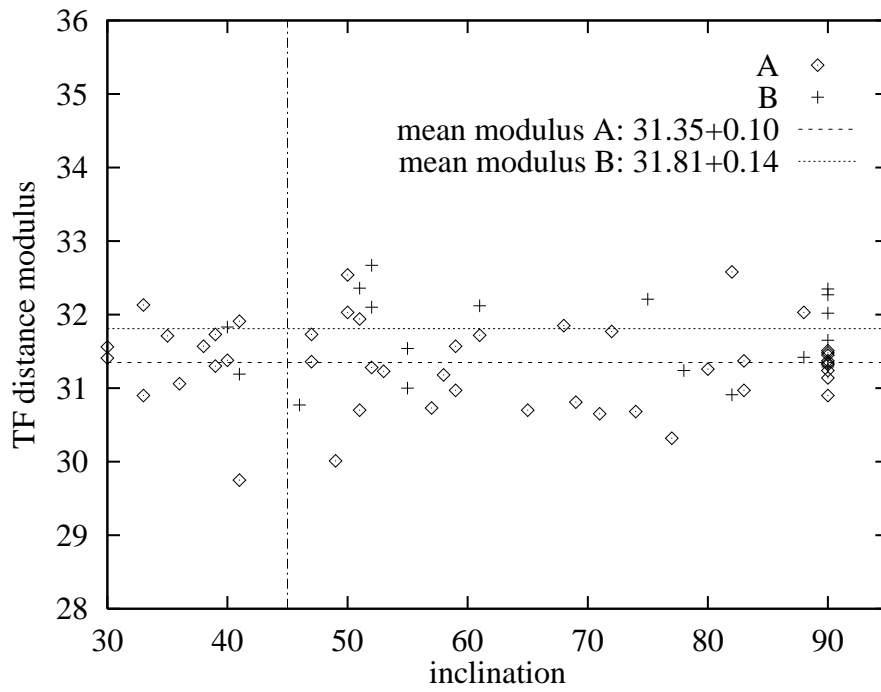


Fig. 7.— TF distance of the fiducial sample as a function of inclination. Also shown are the spirals with $30^\circ < i < 45^\circ$ (on the left side of the vertical line).

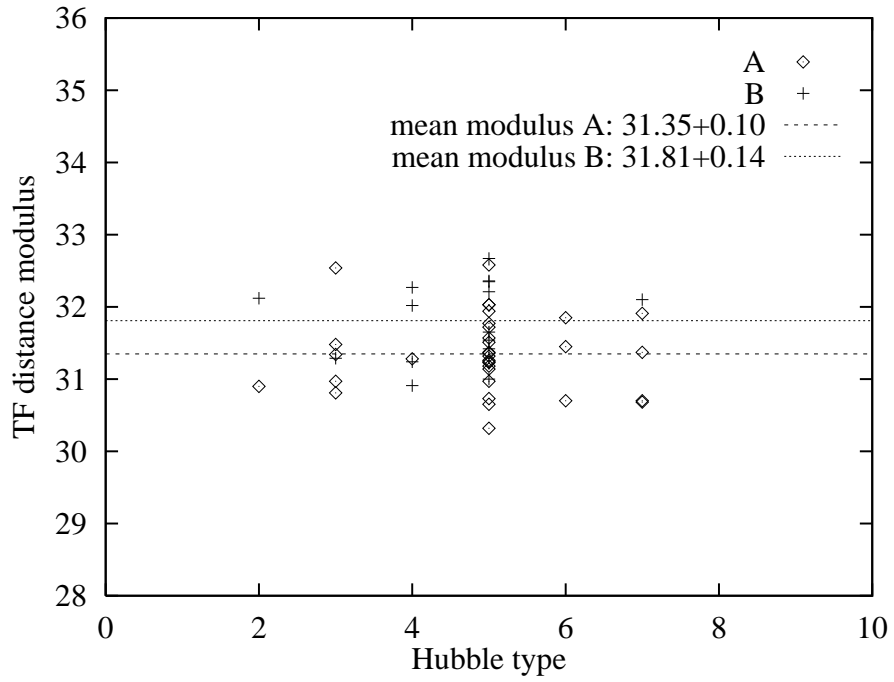


Fig. 8.— TF distance of the fiducial sample as a function of Hubble type.

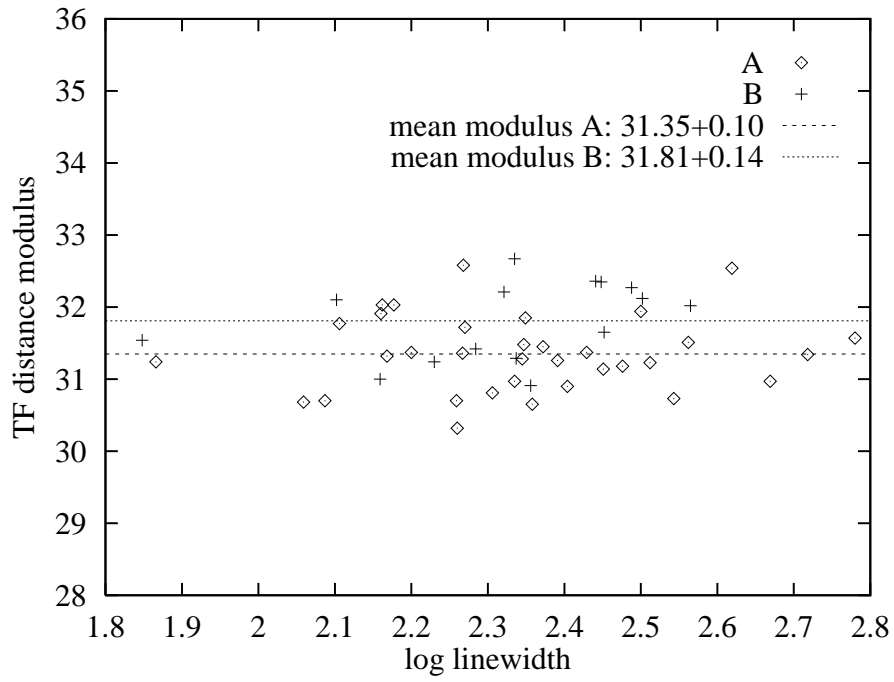


Fig. 9.— TF distance of the fiducial sample as a function of line width.

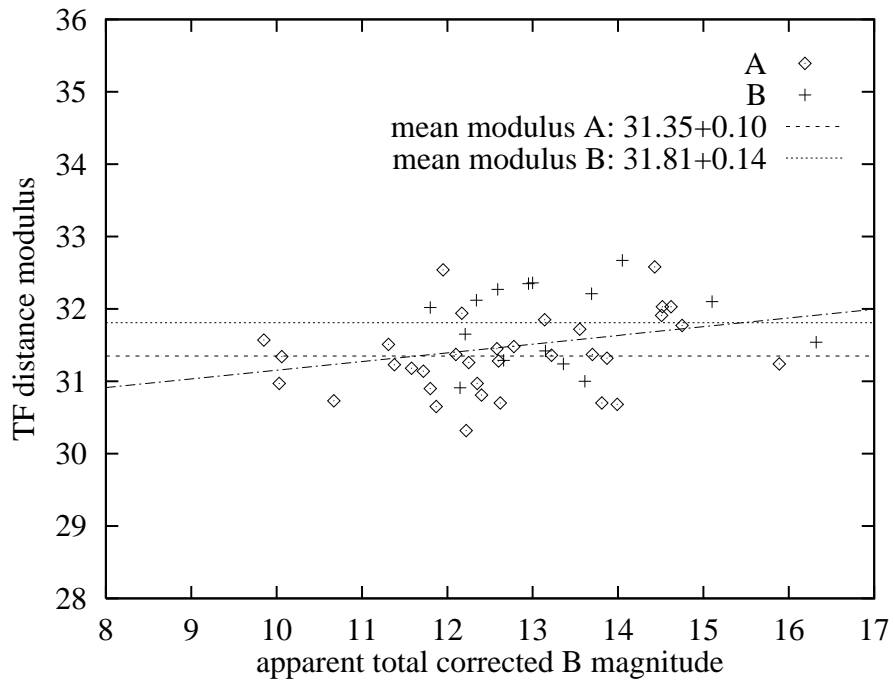


Fig. 10.— TF distance of the fiducial sample as a function of apparent magnitude. Due to the depth of the cluster of about $\pm 0^m.4$, galaxies on the near side are slightly brighter than those on the far side.

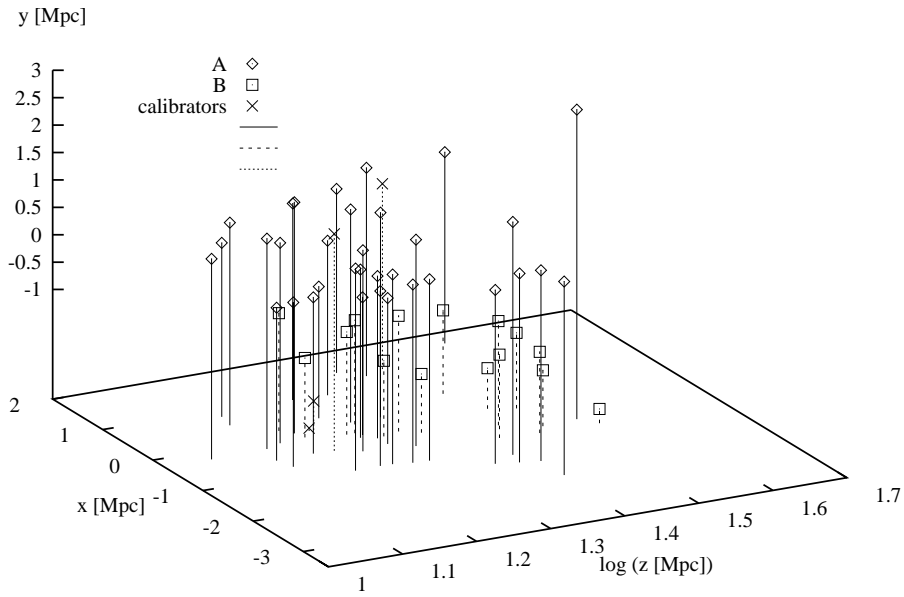


Fig. 11.— 3-D view of the Virgo cluster calculated from Tully-Fisher distances. The x - y plane corresponds to the sky as seen from the Sun (the units being transformed into linear distances at the respective Virgo galaxy distance), the z -axis shows the TF distance in logarithmic units ($\log d_{\text{TF}}[\text{Mpc}]$). The Sun is to the left, M87 and the Sun is at $x = y = 0$. The calibrators among the Virgo galaxies are shown at their respective Cepheid distance. The galaxy on the extreme right front (at the largest z -distance) is IC 3033 (see Sect. 7).

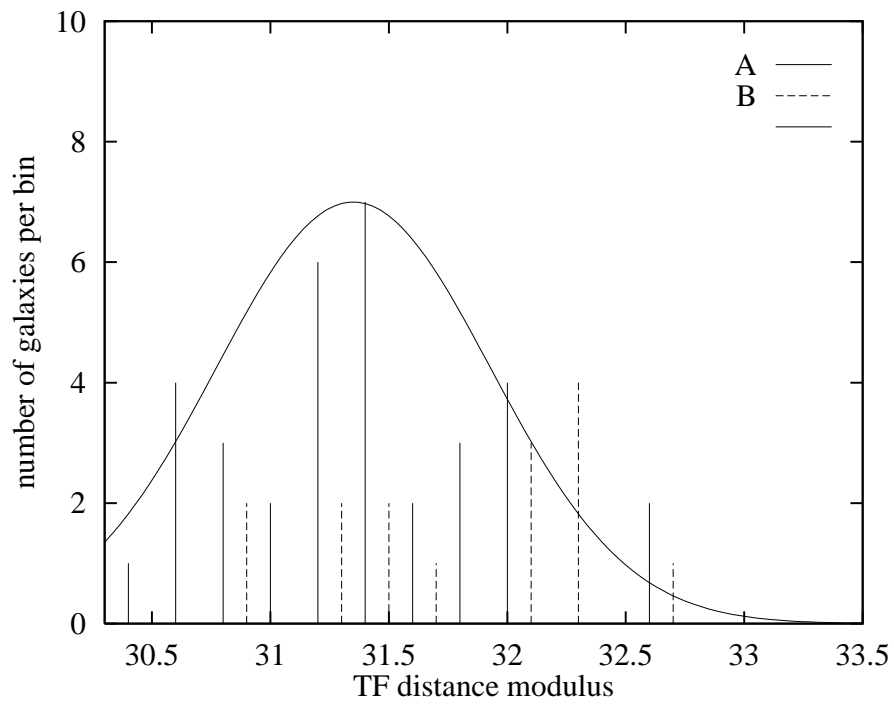


Fig. 12.— Distribution of the individual distance moduli of subclusters A and B. As a crude approximation a Gaussian was fitted to the data of A; subcluster B has a bimodal rather than Gaussian distribution.

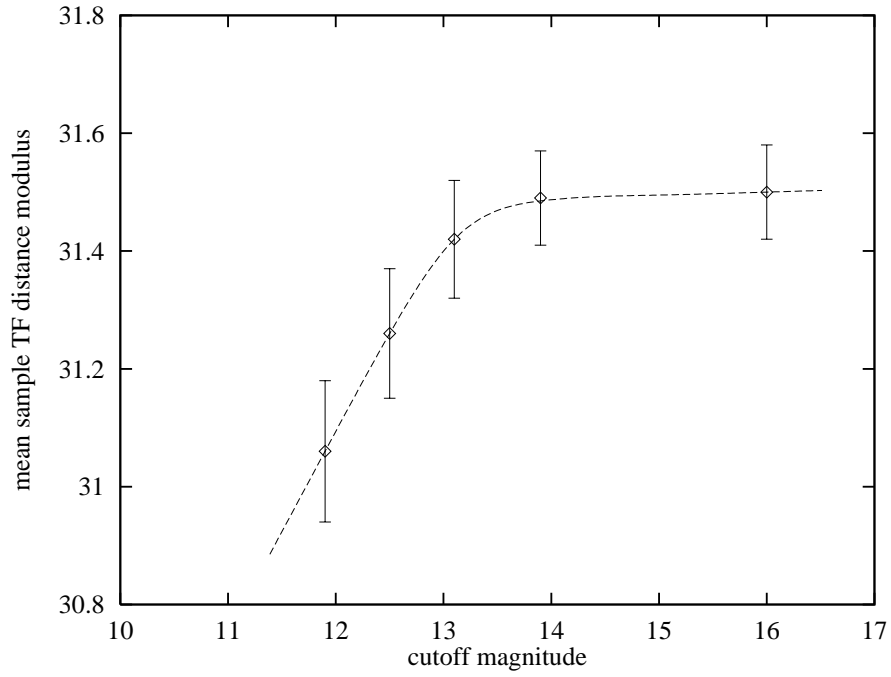


Fig. 13.— The Teerikorpi cluster incompleteness bias for the fiducial sample of the Virgo cluster. The apparent TF distance modulus is a function of the apparent-magnitude cutoff of the sample. The asymptotic value, which is the distance of the cluster, is only reached if the sample of cluster galaxies is *complete* and reaches deep into the luminosity function (Sandage et al. 1995). The dashed line is a nonparametric fit through the data points using thin plate splines and regularisation.

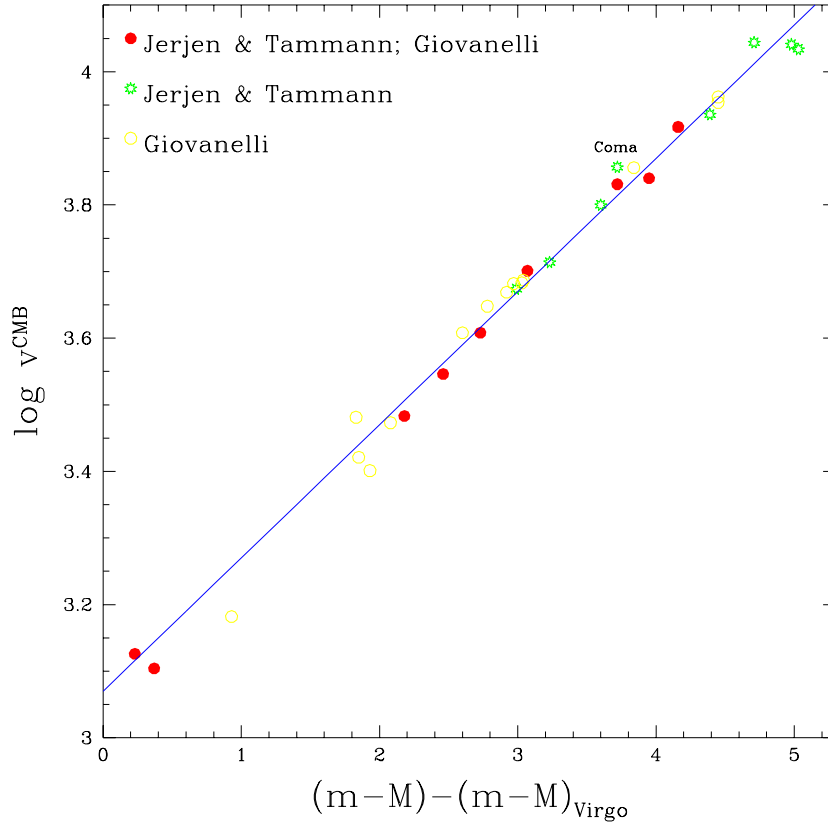


Fig. 14.— Hubble diagram of 31 clusters with known relative distances. The data were taken from Jerjen & Tammann (1993; asterisks) and Giovanelli (1996; open circles). Nine clusters are listed in both sources (filled circles). The abscissa gives the distance modulus relative to the Virgo cluster. The ordinate is the log of the recession velocity referred to the CMB. For “local” clusters with $v_0 < 3000 \text{ km s}^{-1}$ the velocities are referred to the centroid of the Local Group and corrected for Virgocentric infall, following the precepts of Federspiel et al. (1994).

TABLE 1
DISTANCE DETERMINATIONS OF LMC

object	method	$(m - M)^0$	zeropoint	Source
ring of SN1987A	geometry	18.56 ± 0.05	–	Panagia et al. 1996
RR Lyr	P-L- $\left[\frac{Fe}{H} \right]$	18.60 ± 0.11	Sandage 1993	Walker 1993; Tammann 1996
red giants	tip of CMD	18.43 ± 0.15	Sandage 1993	Lee et al. 1993; Tammann 1996
Cepheids (<i>BVIJHK</i>)	Baade-Wesselink	18.57 ± 0.15	–	Laney & Stobie 1992
Cepheids	P-L relation	18.59 ± 0.15	Hyades	Sandage & Tammann 1971
Cepheids	P-L relation	18.47 ± 0.15	Pleiades	Feast & Walker 1987
Cepheids	P-L relation	18.57 ± 0.10	Pleiades	Feast 1995
Cepheids	P-L relation	18.42 ± 0.11	Pleiades	Böhm-Vitense 1997
Cepheids	P-L relation	18.70 ± 0.10	trig. parallaxes	Feast & Catchpole 1997
Mira variables	P-L relation	18.54 ± 0.10	trig. parallaxes	van Leeuwen et al. 1997
Cepheids	<i>I</i> Baade-Wesselink	$18.58 \pm (0.02)$	stellar radii	Di Benedetto 1997
Cepheids	P-L relation	18.57 ± 0.11	trig. parallaxes	Madore & Freedman 1997
mean:		18.56 ± 0.03		

TABLE 2
DATA FOR THE CALIBRATORS

Name	Hubble- type	$B_T^{0,i}$ mag	A^i mag	A^0 mag	$(m - M)$ mag	Source	M_B mag	error mag	i_{RC3} °	$\log w$ H&R	$\log w$ LEDA	error
(1)	(2)	(3)	(4)	(5)	(6)	(7)	(8)	(9)	(10)	(11)	(12)	(13)
N 224 (M 31)	3	3.36	0.67	0.33	24.44	1†	-21.08	0.24	78	2.739	2.728	0.050
N 300	5	8.49	0.21	0.02	26.67	1	-18.18	0.20	44	2.344	2.296	0.036
N 598 (M 33)	5	5.73	0.35	0.19	24.63	1	-18.90	0.17	55	2.373	2.357	0.053
N 925	5	10.04	0.38	0.27	29.84	2	-19.80	0.22	58	2.395	2.382	0.031
N 1365	4	9.94	0.38	0.00	31.30	3	-21.36	0.15	59	2.655	2.648	0.019
N 2090	5	11.52	0.47	0.00	30.41	4	-18.89	0.30	63	2.526	2.503	0.021
N 2403	5	8.38	0.38	0.17	27.51	1	-19.13	0.29	62	2.484	2.415	0.033
N 3031 (M 81)	3	7.34	0.39	0.16	27.80	5	-20.46	0.29	65	2.697	2.667	0.031
N 3351 (M 95)	3	10.24	0.24	0.05	30.01	6	-19.77	0.20	50	2.546	2.538	0.029
N 3368 (M 96)	2	9.85	0.20	0.06	30.32	7	-20.47	0.20	50	2.656	2.649	0.041
N 3621	5	9.40	0.36	0.42	28.95	8	-19.55	0.23	57	2.518	2.509	0.024
N 4321 (M 100)	5	9.88	0.11	0.06	31.04	9	-21.16	0.26	29*	2.733	2.725	0.100
N 4536	4	10.62	0.54	0.00	31.11	10	-20.49	0.16	66	2.546	2.548	0.019
N 4639	3	11.95	0.23	0.06	32.00	11	-20.05	0.26	50	2.626	2.617	0.037
N 5204	7	11.43	0.30	0.00	29.34	12	-17.87	0.28	57	2.146	2.131	0.036
N 5457 (M 101)	5	8.31	0.00	0.00	29.34	12	-21.03	0.18	22*	2.680	2.665	0.100
N 5585	7	10.94	0.26	0.00	29.34	12	-18.36	0.27	52	2.290	2.260	0.055
N 7331	3	9.39	0.61	0.35	30.94	13	-21.57	0.25	75	2.740	2.725	0.014

TABLE 3
DATA FOR VIRGO CLUSTER GALAXIES

Name	sub- group	Hubble- type	$B_T^{0,i}$ mag	error mag	A_{RC3}^i mag	A_{RSA}^i mag	A_{RC3}^0	i_{RC3} °	$\log w$ H&R	$\log w$ LEDA	error
(1)	(2)	(3)	(4)	(5)	(6)	(7)	(8)	(9)	(10)	(11)	(12)
Members of “big A” or “B ($r = 2.4^\circ$)”, $i > 45^\circ$, (“fiducial sample”)											
I3033	A	5	14.62	.21	.27	.44	.03	50	2.276	2.162	0.035
N4192	A	3	10.03	.27	.76	1.17	.16	83	2.675	2.669	0.023
U7249	A	5	14.75	.24	.66	.67	.02	72	2.130	2.106	0.067
I3059	A	7	14.51	.20	.17	.39	.02	41	2.187**	2.160	0.078
I3066	A	5	14.52	.29	1.03	.87	.02	88	2.194**	2.177	0.073
N4206	A	5	11.72	.30	1.08	.87	.02	90	2.450	2.451	0.041
N4212	A	5	11.38	.22	.32	.46	.14	53	2.558	2.512	0.059
N4216	A	3	10.06	.27	.91	1.31	.02	90	2.732	2.718	0.023
N4222	A	6	12.58	.33	1.26	.87	.02	90	2.367	2.372	0.048
N4237	A	5	12.17	.21	.29	.45	.05	51	2.540	2.500	0.068
I3105	A	7	13.99	.25	.70	.73	.04	74	2.068	2.059	0.082
N4294	A	5	11.87	.24	.63	.65	.03	70	2.362	2.358	0.031
N4298	A	5	11.58	.22	.38	.50	.08	57	2.500	2.476	0.037
N4302	A	5	11.31	.31	1.11	.87	.08	90	2.567	2.562	0.032
N4307	B	4	11.80	.28	.98	.87	.00	90	2.588	2.565	0.032
N4313	A, X	2	11.80	.25	.73	1.22	.01	90	2.422	2.404	0.045
N4316	B	4	12.59	.29	1.03	.87	.00	90	2.500	2.488	0.037
N4330	A, X	7	12.10	.28	.97	.87	.02	82	2.464	2.429	0.040
N4353	B, X	5	14.05	.21	.30	.46	.00	52	2.352	2.335	0.045
N4356	B, X	5	12.95	.29	1.06	.87	.00	90	2.486	2.448	0.041
I3298	A	5	14.43	.27	.92	.82	.01	81	2.299	2.268	0.057
N4380	B, X	2	12.34	.21	.32	.78	.00	60	2.524	2.502	0.028
I3311	A, X	5	13.70	.31	1.12	.87	.06	90	2.260	2.200	0.070
I3322A	B, X	5	12.21	.33	1.33	.87	.00	90	2.442	2.452	0.040
I3322	B, X	5	13.15	.29	1.03	.87	.00	88	2.338	2.284	0.058
N4396	A, X	5	12.22	.26	.80	.75	.04	77	2.279	2.260	0.052
N4413	A, X	4	12.60	.21	.28	.45	.11	51	2.316	2.345	0.052
V 952	B, X	5	16.32	.21	.33	.47	.00	54	1.891**	1.848	0.086
I3365	A, X	6	13.81	.23	.50	.58	.03	64	2.155	2.087	0.054
I3371	A, X	5	13.88	.37	1.54	.87	.02	90	2.186*	2.168	0.075
N4445	B, X	3	12.66	.28	1.01	1.33	.00	90	2.356	2.337	0.052
U7590	B, X	4	13.36	.25	.76	.74	.00	78	2.241	2.230	0.058
N4451	B, X	5	13.00	.21	.29	.45	.00	51	2.498	2.441	0.062
I3392	A, X	3	12.40	.23	.51	.93	.08	69	2.340	2.306	0.034
I3414	B, X	5	13.61	.21	.33	.47	.00	54	2.182	2.159	0.023
N4466	B, X	5	13.69	.25	.73	.71	.00	75	2.373	2.321	0.041
N4498	A, X	5	12.35	.22	.41	.52	.03	59	2.373	2.335	0.023
I 797	A, X	5	13.22	.21	.24	.42	.09	47	2.292	2.267	0.060
N4501	A, X	5	9.85	.22	.41	.52	.10	59	2.793	2.780	0.047
N4522	B, X	4	12.15	.26	.84	.78	.00	81	2.377	2.356	0.046
I3517	B, X	7	15.10	.21	.28	.46	.00	51	2.130	2.102	0.027
V1605	A, X	5	15.89	.32	1.26	.87	.00	90	1.900**	1.866	0.139
N4595	A, X	7	12.62	.21	.26	.45	.03	50	2.286	2.259	0.046
N4607	A, X	3	12.78	.28	.88	1.29	.09	90	2.365	2.347	0.051
N4633	A	6	13.14	.23	.57	.62	.04	68	2.338	2.349	0.024
N4634	A	5	12.25	.27	.87	.79	.04	80	2.444	2.391	0.041
N4639	A, X	3	11.95	.21	.23	.66	.06	49	2.626	2.619	0.086
N4654	A, X	5	10.67	.22	.36	.49	.07	56	2.571	2.543	0.046
I3742	A	5	13.55	.22	.43	.54	.07	61	2.316	2.270	0.019
HI-truncated galaxies (Guhathakurta et al. 1988)											
N4388	A, X	2	10.85	.27	.79	1.29	.12	90	2.566	2.572	0.031
N4402	A, X	3	11.70	.27	.76	1.17	.13	83	2.446	2.440	0.039
N4438	A, X	3	10.33	.24	.59	1.01	.10	73	2.606	2.558	0.016
N4450	A	2	10.71	.20	.16	.60	.03	44	2.534	2.624	0.119
N4569	A, X	2	9.75	.22	.42	.89	.09	68	2.591	2.575	0.016
peculiar or interacting galaxies (Binggeli et al. 1985)											
I3044	A	5	13.58	.24	.57	.61	.09	68	2.190	2.154	0.052
N4568 ¹	A, X	5	11.13	.23	.54	.60	.01	66	2.589	2.565	0.016

TABLE 3—Continued

Name	sub- group	Hubble- type	$B_T^{0,i}$ mag	error mag	A_{RC3}^i mag	A_{RSA}^i mag	A_{RC3}^0	i_{RC3} °	log w H&R	log w LEDA	error
(1)	(2)	(3)	(4)	(5)	(6)	(7)	(8)	(9)	(10)	(11)	(12)
members of A, B with $30^\circ < i < 45^\circ$											
U7200	A	8	14.13	.20	.12	.18	.05	40	0.000 [†]	0.000	0.000
V 132	A	7	16.37	.20	.17	.39	.02	41	1.677*	1.585	0.147
N4254	A	5	10.24	.20	.09	.33	.11	30	2.736	2.702	0.260
N4321	A, X	4	9.89	.20	.10	.34	.06	32	2.747	2.679	0.232
I3258	A, X	5	13.40	.20	.09	.33	.08	30	2.310	2.270	0.192
N4351	A, X	5	12.76	.21	.26	.43	.01	44	2.236	2.138	0.041
N4390	A, X	4	13.18	.20	.10	.34	.00	32	2.352	2.384	0.189
N4411A	B, X	5	13.38	.20	.03	.30	.00	17 ²	2.405	2.484	0.410
I3476	A, X	5	12.95	.21	.12	.35	.12	34	2.405	2.355	0.168
I3483 ³	A, X	3	15.52	.20	.17	.59	.01	42	2.348	2.276	0.097
N4519	B, X	5	12.18	.20	.17	.38	.00	40	2.446	2.484	0.142
N4535	B, X	5	10.37	.20	.22	.41	.00	44	2.606	2.591	0.107
I3520	A, X	6	14.68	.21	.24	.42	.08	42	2.190	2.109	0.044
N4540	A, X	6	12.23	.20	.16	.38	.05	39	2.318	2.412	0.134
N4548	A, X	3	10.75	.20	.14	.56	.07	38	2.663	2.612	0.164
N4571	A, X	5	11.69	.20	.08	.32	.06	27 ⁴	2.548	2.534	0.271
N4579	A, X	2	10.21	.21	.12	.56	.15	39	2.787	2.753	0.170
U7795	B, X	8	14.54	.20	.14	.19	.00	41	2.064	2.053	0.059
N4647	A, X	5	11.75	.20	.15	.37	.04	38	2.505	2.507	0.157
N4689	A, X	5	11.41	.20	.14	.36	.05	36	2.580	2.482	0.170
galaxies outside A or B but within X-ray contours:											
N4252	Z, X	5	13.96	.27	.92	.82	.00	81	2.212**	2.196	0.067
V 297	Z, X	5	14.00	.31	1.22	.87	.00	90	2.239*	2.224	0.066
N4273	W, X	5	12.09	.21	.30	.46	.00	52	2.558**	2.558	0.066
V 415	W, X	7	14.57	.21	.37	.52	.00	58	2.163**	2.111	0.036
U7423	X, X	7	15.23	.21	.32	.48	.00	54	2.212	2.231	0.022
I3225	W, X	6	13.79	.24	.71	.70	.00	73	2.353**	2.333	0.038
I3229	X, X	5	14.39	.26	.84	.77	.00	78	2.161	2.120	0.077
N4343	X, X	3	12.37	.25	.75	1.15	.00	82	2.534	2.535	0.031
I3259	X, X	5	13.85	.21	.39	.51	.00	58	2.305	2.288	0.015
N4470 ³	Z, X	5	12.81	.20	.21	.40	.00	44	2.324	2.291	0.080
I 800 ³	Z, X	5	13.81	.21	.21	.40	.05	44	2.258	2.137	0.058
U7802	Z, X	5	13.86	.30	1.11	.87	.00	90	2.238	2.216	0.068
N4591	Z, X	3	13.60	.22	.41	.83	.00	63	2.603	2.538	0.021
N4651	Y, X	5	11.09	.21	.27	.44	.03	50	2.718	2.685	0.088
N4746	Y, X	3	12.57	.25	.72	1.13	.07	80	2.543	2.535	0.029
galaxies outside A or B and outside X-ray contours											
I 755	Y	3	12.79	.31	1.21	1.33	.00	90	2.316	2.304	0.056
U7016	Y	2	13.60	.26	.81	1.31	.01	90	0.000 [†]	0.000	0.000
N4064	Y	5	11.60	.24	.60	.63	.02	69	2.318	2.299	0.032
N4067	Y	3	13.12	.20	.19	.62	.00	45	2.587	2.556	0.107
N4082	Y	5	14.69	.20	.00	.28	.19	0	0.000 [†]	0.000	0.000
U7133	Y	7	15.00	.21	.26	.45	.03	50	2.354	2.387	0.059
U7209	M	3	13.12	.21	.23	.66	.03	49	2.549	2.515	0.078
N4178	Z	5	11.22	.24	.68	.68	.00	72	2.491	2.454	0.024
N4180	W	3	12.89	.23	.58	.99	.00	73	2.645	2.625	0.014
N4189	M	5	12.27	.21	.21	.40	.03	44	2.672	2.586	0.113
N4193	M	5	12.68	.22	.48	.56	.02	63	2.602	2.576	0.025
N4197	Z	6	12.29	.30	1.15	.87	.00	90	2.442	2.427	0.043
I3061	M	5	13.13	.31	1.06	.87	.14	90	2.509	2.470	0.038
N4207	Z	6	13.05	.22	.43	.54	.00	60	2.393	2.346	0.022
I3074	Z	7	13.58	.30	1.15	.87	.00	90	2.371	2.335	0.052
I3099	M	6	13.68	.32	1.21	.87	.04	90	2.398	2.343	0.051
I 776	Z	6	13.98	.21	.32	.47	.00	54	2.350	2.332	0.037
U7387	W	6	13.59	.36	1.44	.87	.07	90	2.411**	2.400	0.045
N4289	W	4	13.05	.36	1.48	.87	.02	90	2.555	2.554	0.032
V 737	W	7	14.44	.24	.59	.66	.03	70	2.215	2.207	0.047
N4376	Z	6	13.51	.21	.31	.46	.00	53	2.236	2.250	0.031

TABLE 3—*Continued*

Name	sub- group	Hubble- type	$B_T^{0,i}$ mag	error mag	A_{RC3}^i mag	A_{RSA}^i mag	A_{RC3}^0 (8)	i_{RC3} °	log w H&R	log w LEDA	error
(1)	(2)	(3)	(4)	(5)	(6)	(7)	(8)	(9)	(10)	(11)	(12)
U7522	W	5	13.02	.35	1.42	.87	.03	90	2.495**	2.486	0.037
N4405	Z	5	12.70	.21	.29	.45	.03	51	2.674	2.236	0.038
N4420	W	5	12.38	.22	.48	.56	.00	63	2.344	2.338	0.020
N4423	Z	7	12.93	.29	1.08	.87	.00	87	2.233	2.232	0.065
U7579	W	6	14.24	.30	1.09	.87	.00	87	2.377	2.355	0.050
N4455	Y	5	12.23	.27	.81	.76	.06	77	2.188	2.098	0.079
N4480	W	3	12.73	.22	.41	.83	.01	63	2.619	2.563	0.023
I3474	W	7	13.61	.33	1.30	.87	.00	90	2.179	2.150	0.077
U7697	Y	5	13.87	.31	1.09	.87	.12	90	2.326	2.304	0.056
N4527	W	3	10.79	.23	.57	.98	.02	72	2.606	2.592	0.015
N4533	W	6	13.48	.30	1.13	.87	.00	90	2.254**	2.239	0.064
N4536	W	5	10.63	.23	.52	.59	.00	65	2.566**	2.548	0.016
N4544	S	5	13.20	.26	.75	.72	.05	75	2.305	2.314	0.044
N4713	Y	5	11.89	.21	.30	.46	.00	52	2.356	2.355	0.049
U8114	Y	5	14.62	.23	.55	.61	.00	67	2.182	2.176	0.047
N4758	Y	3	12.67	.27	.87	1.27	.01	90	2.297	2.282	0.059
U8032	Y	5	13.62	.27	.89	.80	.00	80	0.000 [†]	0.000	0.000
I3881	Y	5	12.66	.29	.93	.83	.12	82	2.318	2.310	0.052
N4808	Y	5	11.78	.23	.57	.61	.00	68	2.467	2.391	0.022
U8085	Y	3	13.71	.27	.87	1.27	.04	90	2.387	2.364	0.049

NOTE.—¹ interacting pair N4567/8 (VV219)
² N4411A: Fouqué et al. (1990) give $i = 30^\circ$
³ peculiar galaxy (Binggeli et al. 1985)
⁴ N4571: Fouqué et al. (1990) give $i = 30^\circ$

TABLE 4

COMPARISON OF TF PARAMETERS AND THE TF DISTANCE TO THE VIRGO CLUSTER FOR DIFFERENT SETS OF INPUT PARAMETERS [CF. EQ. (1)]

solution	slope	intercept at $\log w = 2.3$		dispersion		n_{Virgo}	$(m - M)_{\text{Virgo}}$	error
		Virgo	calibrators	Virgo	calibrators			
(1)	(2)	(3)	(4)	(5)	(6)	(7)	(8)	(9)
1	-6.969	13.13	-18.37	0.57	0.44	49	31.50	0.09
2	-7.071	13.33	-18.23	0.61	0.48	49	31.57	0.08
3	-7.152	13.13	-18.35	0.60	0.43	67	31.48	0.07
4	-6.551	13.06	-18.94	0.65	0.44	35	32.00	0.11
5	-7.311	13.11	-18.51	0.62	0.39	49	31.63	0.10
6	-7.371	13.34	-18.40	0.65	0.44	49	31.74	0.09
7	-7.454	13.09	-18.51	0.65	0.38	67	31.60	0.08
8	-6.925	13.15	-18.39	0.56	0.43	49	31.54	0.09
mean over 1-7							31.65 ± 0.17	

NOTE.—Parameters for the different solutions:

1. Magnitudes and A^i , A^0 from RC3, $\log w$ from LEDA
2. Magnitudes and from A^i , A^0 from RC3, $\log w$ from Huchtmeier and Richter (1989)
3. Like 1, but including all members of subclusters A+B with $i > 30^\circ$
4. Like 1, but using the X-ray sample (excluding seven galaxies in the SW corner)
5. Magnitudes and A^0 from RC3, A^i from RSA, $\log w$ from LEDA
6. Magnitudes and A^0 from RC3, A^i from RSA, $\log w$ from Huchtmeier and Richter (1989)
7. Like 5, but including all members of subclusters A+B with $i > 30^\circ$
8. Magnitudes and A^i from RC3, $A^0 = 0$, $\log w$ from LEDA

TABLE 5

A COMPARISON OF CEPHEID AND TULLY-FISHER DISTANCES (TABLE 4, SOLUTION 1)

galaxy	v_{LG}	$(m - M)_{\text{Cepheid}}$	$(m - M)_{\text{TF}}$	$\Delta(m - M)$	subcluster
N4321	1464	31.04 ± 0.26	31.21 ± 0.40	-0.17 ± 0.50	A
N4496A ¹⁾	1568	31.13 ± 0.10	30.67 ± 0.40	0.46 ± 0.44	W
N4536	1646	31.11 ± 0.05	30.72 ± 0.40	0.39 ± 0.43	W
N4639	860	32.00 ± 0.23	32.53 ± 0.40	-0.53 ± 0.49	A

NOTE.—¹⁾ The magnitude may be disturbed by N 4496B

TABLE 6
EXTERNAL ERRORS OF THE VIRGO CLUSTER MODULUS

error source	error
zeropoint of the Cepheid P-L relation	0^m10
adopted slope of the TF relation	0^m10
precepts of weighting the data	0^m08
weight of the X-ray sample	0^m10
correction for internal absorption	0^m10
intrinsic differences between calibrators and Virgo galaxies	0^m05
inclination difference between calibrators and Virgo galaxies	0^m05
estimated total external error	0^m23

TABLE 7

THE VALUES OF H_0 CALCULATED FOR SUBCLUSTERS A AND B SEPARATELY

	n	v_{220}	$(m - M)$	r (Mpc)	H_0
A	34	1164 ± 67	31.35 ± 0.1	18.6 ± 0.9	63 ± 4
B	15	1111 ± 76	31.81 ± 0.1	23.0 ± 1.6	48 ± 5